A phosphatase threshold sets the level of Cdk1 activity in early mitosis in budding yeast

Stacy L. Harvey[a], Germán Enciso[b,d], Noah E. Dephoure[c], Steven P. Gygi[c], Jeremy Gunawardena[b], and Douglas R. Kellogg[a,*]

[a]Department of Molecular, Cell, and Developmental Biology, University of California, Santa Cruz, CA 95064

[b]Department of Systems Biology, Harvard Medical School, Boston, MA 02115

[c]Department of Cell Biology, Harvard Medical School, Boston, MA 02115

[d]Present address: Department of Mathematics, University of California, Irvine, CA 92697

*Correspondence: kellogg@biology.ucsc.edu

Running Head: PP2A-dependent modulation of Cdk1 activity

ABSTRACT

Entry into mitosis is initiated by synthesis of cyclins, which bind and activate cyclin-dependent kinase 1 (Cdk1). Cyclin synthesis is gradual, yet activation of Cdk1 occurs in a stepwise manner: a low level of Cdk1 activity is initially generated that triggers early mitotic events, which is followed by full activation of Cdk1. Little is known about how stepwise activation of Cdk1 is achieved. A key regulator of Cdk1 is the Wee1 kinase, which phosphorylates and inhibits Cdk1. Wee1 and Cdk1 show mutual regulation: Cdk1 phosphorylates Wee1, which activates Wee1 to inhibit Cdk1. Further phosphorylation events inactivate Wee1. We discovered that a specific form of protein phosphatase 2A ($PP2A^{Cdc55}$) opposes the initial phosphorylation of Wee1 by Cdk1. In vivo analysis, in vitro reconstitution and mathematical modeling suggest that $PP2A^{Cdc55}$ sets a threshold that limits activation of Wee1, thereby allowing a low constant level of Cdk1 activity to escape Wee1 inhibition in early mitosis. These results define a new role for $PP2A^{Cdc55}$ and reveal a systems-level mechanism by which dynamically opposed kinase and phosphatase activities can modulate signal strength.

INTRODUCTION

Mitosis is an intricate and precisely ordered series of events that results in chromosome segregation and cell division. The key molecular event that initiates mitosis is activation of cyclin-dependent kinase 1 (Cdk1) (Morgan, 2007). Cdk1 activation requires binding of mitotic cyclins, which are synthesized anew each cell cycle and accumulate gradually during entry into mitosis. In human somatic cells and *Xenopus* eggs activation of Cdk1 occurs in a stepwise manner: a low constant level of Cdk1 activity is initially generated in early mitosis, which is followed by full, switch-like activation of Cdk1 (Solomon *et al.*, 1990; Pomerening *et al.*, 2005; Lindqvist *et al.*, 2007; Deibler and Kirschner, 2010). Thus, a

gradually increasing signal generated by cyclin synthesis is converted to stepwise activation of Cdk1. This also appears to be true in budding yeast, where a low threshold of Cdk1 activity is required for initiation of mitotic spindle assembly and a higher threshold initiates spindle elongation (Rahal and Amon, 2008). Stepwise activation of Cdk1 helps ensure that mitotic events occur in the proper order (Deibler and Kirschner, 2010). More generally, the molecular mechanisms by which a gradually increasing signal is converted to a step function are of great interest.

The Wee1 kinase and the Cdc25 phosphatase play important roles in modulation of Cdk1 activity during entry into mitosis (Nurse, 1975; Russell and Nurse, 1986, 1987). Wee1 phosphorylates Cdk1 on a conserved tyrosine, thereby inhibiting Cdk1 and delaying entry into mitosis (Gould and Nurse, 1989). Cdc25 promotes entry into mitosis by removing the inhibitory phosphate (Gautier *et al.*, 1991; Kumagai and Dunphy, 1991). Wee1 and Cdc25 are thought to contribute to the abrupt, switch-like activation of Cdk1 via feedback loops in which Cdk1 inhibits Wee1 and activates Cdc25 (Izumi *et al.*, 1992; Kumagai and Dunphy, 1992; Hoffman *et al.*, 1993; Izumi and Maller, 1993; Tang *et al.*, 1993; Mueller *et al.*, 1995). They also enforce cell cycle checkpoints that delay entry into mitosis until previous events have been completed (Rupes, 2002; Kellogg, 2003; Karlsson-Rosenthal and Millar, 2006; Keaton and Lew, 2006).

Recent work established that Wee1 plays an important role in the mechanism that generates a low plateau of Cdk1 activity in early mitosis. In vertebrate cells, low level activation of Cdk1 in early mitosis occurs in the presence of active Wee1 and is dependent upon Wee1 (Deibler and Kirschner, 2010). These seemingly paradoxical findings suggest that Wee1 does not act in a simple all-or-nothing manner to inhibit Cdk1. Rather, it appears that the activity of Wee1 can be restrained to allow a low level of Cdk1 activity to be generated in early mitosis. A mechanism that restrains Wee1 also appears to operate in budding yeast because two key early mitotic events occur in the presence of active Wee1. First, a low level of Cdk1 activity in early mitosis initiates a positive feedback loop that promotes transcription of mitotic cyclins (Amon *et al.*, 1993). Wee1 is present in excess when mitotic cyclins first accumulate and is capable of inhibiting both nuclear and cytoplasmic pools of Cdk1 (Sreenivasan and Kellogg, 1999; Harvey and Kellogg, 2003; Harvey *et al.*, 2005; Keaton *et al.*, 2008). Thus, initiation of the positive feedback loop requires a mechanism by which Cdk1 can be activated in the presence of Wee1. Second, checkpoints that block nuclear division via activation of Wee1 cause an arrest at the short spindle stage of early mitosis (Carroll *et al.*, 1998; Sreenivasan and Kellogg, 1999; Theesfeld *et al.*, 1999). Since formation of a short spindle requires a low level of mitotic Cdk1 activity, this further suggests that low level activation of Cdk1 occurs in the presence of active Wee1 (Fitch *et al.*, 1992; Rahal and Amon, 2008).

How is a low level of Cdk1 activity generated in early mitosis in the presence of active Wee1? Also, how is a low constant level of Cdk1 activity maintained in early mitosis as cyclin levels rise? Investigations into the mechanisms that regulate Wee1 and Cdk1 during entry into mitosis have provided clues. In budding yeast, Cdk1 associated with the mitotic cyclin Clb2 directly phosphorylates Wee1, which stimulates Wee1 to bind, phosphorylate and inhibit Cdk1 (Harvey *et al.*, 2005). Thus, Cdk1 activates its own inhibitor. A similar mechanism acts in human cells, which suggests that it is conserved (Deibler and Kirschner, 2010). When Cdk1 activity is inhibited in vivo, Wee1 undergoes rapid, quantitative dephosphorylation, which reveals that phosphorylation of Wee1 by Cdk1 is opposed by a phosphatase (Harvey *et al.*, 2005). After the initial phosphorylation and activation of Wee1 by Cdk1 in early mitosis, further phosphorylation events cause full hyperphosphorylation of Wee1 and dissociation of the Wee1-Cdk1/cyclin complex, which likely represents the inhibition of Wee1 that is necessary for full entry into mitosis (Harvey *et al.*, 2005; Deibler and Kirschner, 2010).

We used these findings as a starting point to investigate how activation of Cdk1 is controlled during entry into mitosis in budding yeast. This led to the discovery that $PP2A^{Cdc55}$ opposes the initial phosphorylation and activation of Wee1 by Cdk1/Clb2 in early mitosis. In vitro reconstitution and mathematical modeling indicate that $PP2A^{Cdc55}$ sets a threshold that limits activation of Wee1 in early mitosis, thereby allowing a low level of Cdk1/Clb2 activity to escape Wee1 inhibition to initiate early mitotic events. Quantitative analysis of Wee1 activation and mathematical modeling further suggest the existence of a systems-level mechanism that keeps the activity of Cdk1/Clb2 at a low constant level as cyclin levels rise during early mitosis.

RESULTS

Cdc28/Clb2 phosphorylates Swe1 on Cdc28 consensus sites

We first carried out an analysis of the mechanism by which mitotic Cdk1/cyclin stimulates activation of Wee1. In budding yeast, Wee1 is referred to as Swe1 and Cdk1 is referred to Cdc28. In previous work, we reconstituted phosphorylation of Swe1 by Cdc28/Clb2 in vitro and used mass spectrometry to map phosphorylation sites (Harvey *et al.*, 2005). We found that Cdc28/Clb2 phosphorylated Swe1 on 8 of 13 possible minimal Cdc28 (Cdk1) consensus sites (S/T-P), as well as 10 non-consensus sites. Most sites were also identified on Swe1 isolated from cells, suggesting that they are physiologically relevant. A *swe1-18A* mutant that lacked these sites eliminated Swe1 hyperphosphorylation in vivo and caused premature entry into mitosis. In addition, the mutant protein failed to form a complex with Cdc28/Clb2. These observations suggested a model in which initial phosphorylation of Swe1 by Cdc28/Clb2 leads to formation of a Swe1-Cdc28/Clb2 complex that drives inhibitory phosphorylation of Cdc28/Clb2.

A limitation of these phosphorylation site mapping experiments is that they were unable to provide information on the stoichiometry of phosphorylation. Thus, it was possible that they identified sites that were phosphorylated at stoichiometries that were too low to be significant. In order to determine which of the 18 sites played a significant role in Swe1 activation by Cdc28/Clb2, we used a more recently developed technique called stable isotope labeling with amino acids in culture (SILAC). This approach allows estimation of the stoichiometry of phosphorylation via use of heavy isotope-labeled unphosphorylated reference peptides (Ong *et al.*, 2002).

We again reconstituted phosphorylation of Swe1 by Cdc28/Clb2 in vitro (Figure 1A). Unphosphorylated and phosphorylated Swe1 were mixed with isotope-labeled unphosphorylated Swe1 and the accumulation of phosphorylated peptides and depletion of the cognate unphosphorylated peptides were monitored. The relative abundance ratios of the unphosphorylated peptides upon phosphorylation were used to calculate site stoichiometry. We performed two independent analyses using peptides generated by digesting Swe1 with trypsin or lysC.

Standard site mapping identified many sites, including most of the sites identified in our previous analysis (Table S1) (Harvey *et al.*, 2005). However, SILAC revealed that the only sites phosphorylated at a measurable stoichiometry were Cdc28 consensus sites (Table 1). An exception was a phosphorylation that occurred within amino acids 159-162, which likely represents Swe1 autophosphorylation on a tyrosine. In two cases, peptides with multiple sites underwent quantitative phosphorylation; however, the SILAC analysis indicates only that these peptides were phosphorylated at high stoichiometry on one or more sites. In these cases, we believe that it is likely that only the Cdc28 consensus sites were phosphorylated at high stoichiometry.

Phosphorylation of Cdc28 consensus sites is required for Swe1 activity in vivo

The SILAC analysis demonstrated that the initial phosphorylation of Swe1 by Cdc28/Clb2 occurs primarily on Cdc28 consensus sites, which suggested that phosphorylation of consensus sites alone drives activation of Swe1 by Cdc28/Clb2. To test whether Cdc28 consensus sites are required for Swe1 activity, we analyzed a mutant version of Swe1 that lacked 8 of the Cdc28 consensus sites identified by mass spectrometry (*swe1-8A*, sites mutated: T45A, S111A, T121A, S133A, T196A, S201A, S263A, and T373A). We previously found that the *swe1-8A* mutant largely eliminated phosphorylation of Swe1 in vivo (Harvey *et al.*, 2005). Moreover, previous work established that loss of Swe1 causes premature entry into mitosis and reduced cell size (Jorgensen *et al.*, 2002; Harvey and Kellogg, 2003; Harvey *et al.*, 2005; Rahal and Amon, 2008). Here, we found that *swe1-8A* caused premature entry into mitosis, as detected by assembly of short mitotic spindles (Figure 1B). The *swe1-8A* mutant also caused reduced cell size and a complete loss of Cdc28 inhibitory phosphorylation (Figures 1C-1D). Finally, the swe1-8A protein failed to form a complex with Cdc28/Clb2 in crude extracts (Figure 1E). The sites mutated in *swe1-8A* were located in the N-terminus far from the kinase domain, and mutation of these sites in the *swe1-18A* mutant did not affect the intrinsic kinase activity of Swe1 (Harvey *et al.*, 2005). A *swe1-13A* mutant that lacked all 13 minimal Cdc28 consensus sites also caused premature entry into mitosis and a reduced cell size (not shown).

We next tested whether the swe1-8A protein was phosphorylated by Cdc28/Clb2 in vitro. We utilized a mutant form of Cdc28 that can not be phosphorylated by Swe1 (cdc28-Y19F), which allowed us to carry out reactions without the complication of Cdc28 inhibition by Swe1. The swe1-8A protein was resistant to phosphorylation by purified cdc28-Y19F/Clb2 (Figure 1F). In contrast, a swe1-10ncs protein that lacked the non-consensus sites identified in our original study was phosphorylated to the same extent as wild-type Swe1, which supported the conclusion that initial phosphorylation of Swe1 by Cdc28/Clb2 occurs on Cdc28 consensus sites (Figure 1F).

These observations are consistent with a model in which Cdc28/Clb2 activates Swe1 and drives formation of the Swe1-Cdc28/Clb2 complex via phosphorylation of Cdc28 consensus sites. Note that only a quantitatively phosphorylated form of Swe1 forms a complex with Cdc28/Clb2 in wild-type cells (Figure 1E and (Harvey *et al.*, 2005)). Based on its electrophoretic mobility, this is likely to correspond to the form of Swe1 that has been quantitatively phosphorylated by Cdc28/Clb2 on consensus sites, which suggests that Swe1 must be quantitatively phosphorylated to bind and inhibit Cdc28. This would be reminiscent of the Cdc28 inhibitor Sic1, which must be quantitatively phosphorylated on 6 minimal Cdc28 consensus sites to bind to Cdc4, which targets Sic1 for destruction (Nash *et al.*, 2001).

To further investigate the mechanism and function of consensus site phosphorylation, we created two additional phosphorylation site mutants in which a smaller number of sites were mutated. In the first mutant, we mutated two sites that correspond to optimal Cdc28 consensus sites (S/TPXXR/K; *swe1-T196A,T373A*). In the second mutant, we mutated two sites that correspond to the minimal Cdc28 consensus site (S/TP; *swe1-S133A,S263A*). In both cases, we chose sites that were quantitatively phosphorylated by Cdc28/Clb2 in the mass spectrometry analysis. There are numerous other phosphorylation site mutants that would be interesting to analyze in this context; these mutants were selected to provide a preliminary analysis of the roles of different classes of sites and to test whether phosphorylation of all sites is necessary for full Swe1 activity. **For both mutants, we analyzed cell size, Cdc28 inhibitory phosphorylation, Swe1 phosphorylation, and formation of the Swe1-Cdc28/Clb2 complex (Figure 2).**

Mutation of the optimal Cdc28 consensus sites (*swe1-T196A,T373A*) caused a small size phenotype similar to a *swe1*Δ and a severe reduction in Cdc28 inhibitory phosphorylation, consistent with loss of Swe1 function (Figures 2A and 2B). Intermediate

phosphorylation forms of the swe1-T196A,T373A protein could be detected, but appeared to be reduced (Figure 2C, compare 50 minute time points). **The swe1-T196A,T373A protein completely failed to form a complex with Cdc28/Clb2 (Figure 2D).**

Mutation of the minimal Cdc28 consensus sites (*swe1-S133A,S263A*) caused reduced cell size (Figure 2A), as well as delayed Cdc28 inhibitory phosphorylation (Figures 2B, compare the 50-60 minute time points in wild-type cells to the same time points in *swe1-S133A,S263A* cells). It also appeared to cause a reduction in Swe1 phosphorylation: most of the swe1-S133A,S263A protein was present in a rapidly migrating form at early time points (Figure 2C, compare 50-60 minute time points). Phosphorylated forms of swe1-S133A, S263A eventually appear, but only at later times when Cdc28/Clb2 accumulates to higher levels. **The swe1-S133A,S263A protein was capable of forming a complex with Cdc28/Clb2.**

The behavior of the *swe1-S133A,S263A* and *swe1-T196A,T373A* mutants indicates that the consensus sites are not all equivalent in terms of function. A model that could explain the behavior of the mutants is that phosphorylation occurs in an ordered and cooperative manner. In this model, phosphorylation of S133 or S263 would occur first and promote subsequent phosphorylation events. **Phosphorylation of T196 and T373 would occur last and stimulate Swe1 activity by promoting formation of the Swe1-Cdc28/Clb2 complex. The model further postulates that phosphorylation of T196 and T373 eventually occurs in the *swe1-S133A,S263A* mutant, but inefficiently and therefore only after Cdc28/Clb2 activity has risen to higher levels. Thus, activation of Swe1 would be delayed in the *swe1-S133A,S263A* mutant, which would explain the observed premature accumulation of active Cdc28 and reduced cell size. The model is consistent with the observation that only the quantitatively phosphorylated form of wild-type Swe1 binds to Cdc28/Clb2 (Figure 1E and (Harvey *et al.*, 2005)).**

Previous work on the fibroblast growth factor receptor found that it undergoes multisite phosphorylation in a sequential and precisely ordered manner, which provides a precedent for a sequential mechanism of Swe1 phosphorylation (Furdui *et al.*, 2006). However, extensive additional experiments will be required to clearly define the mechanism of multisite phosphorylation of Swe1. Although the behavior of the Swe1 phosphorylation site mutants suggests the presence of cooperativity, these observations must be interpreted with caution because phosphorylation has an unpredictable effect on gel mobility: multiple phosphorylations may show no gel shift, while a single phosphorylation may show a large one. Thus, it is not possible to know definitively which sites or how many sites have been phosphorylated based on the electrophoretic mobility of a protein. Quantitative mass spectrometry will be necessary to fully characterize the effects of the mutations on Swe1 phosphorylation.

$PP2A^{Cdc55}$ opposes phosphorylation of Swe1 by Cdc28 in vivo

We next used a candidate approach to search for the phosphatase that opposes phosphorylation of Swe1 by Cdc28. We reasoned that inactivation of the phosphatase should cause premature phosphorylation of Swe1. $PP2A^{Cdc55}$ was a strong candidate because evidence from diverse systems has indicated that it is a key regulator of entry into mitosis and Cdc28 inhibitory phosphorylation. Canonical PP2A is a hetero-trimeric complex composed of a catalytic subunit, a scaffolding subunit, and a regulatory subunit. Cells express multiple regulatory subunits that associate with PP2A in a mutually exclusive manner. In budding yeast, PP2A associates primarily with two regulatory subunits called Rts1 and Cdc55, forming distinct complexes called $PP2A^{Rts1}$ and $PP2A^{Cdc55}$. Inactivation of the catalytic subunit after cells have passed through G1 phase causes defects in entry into mitosis; cells arrest with low levels of mitotic cyclin mRNA and protein, and reduced specific activity of mitotic Cdc28 (Lin and Arndt, 1995). Similarly, *cdc55*Δ causes increased Cdc28

inhibitory phosphorylation, delayed accumulation of mitotic cyclin, and a prolonged delay in early mitosis (Minshull *et al.*, 1996; Yang *et al.*, 2000; Pal *et al.*, 2008). These phenotypes are rescued by *swe1*Δ or *cdc28-Y19F* (Yang *et al.*, 2000; Pal *et al.*, 2008). Conversely, $PP2A^{Cdc55}$ mutants are enhanced by inactivation of Mih1, the budding yeast homolog of Cdc25 (Lin and Arndt, 1995; Pal *et al.*, 2008). For example, *mih1*Δ causes lethality in *cdc55*Δ cells, which is rescued by *swe1*Δ. Together, these observations show that $PP2A^{Cdc55}$ promotes entry into mitosis via regulation of Cdc28 inhibitory phosphorylation. *Xenopus* PP2A also controls entry into mitosis and is thought to regulate Wee1 and Cdc25 (Félix *et al.*, 1990; Kumagai and Dunphy, 1992; Tang *et al.*, 1993; Izumi and Maller, 1995; Mueller *et al.*, 1995; Castilho *et al.*, 2009; Mochida *et al.*, 2009).

To test whether $PP2A^{Cdc55}$ opposes phosphorylation of Swe1, we assayed Swe1 hyperphosphorylation in synchronized *cdc55*Δ *cdc28-Y19F* cells. The *cdc28-Y19F* allele eliminated the mitotic delay caused by *cdc55*Δ, which allowed cell cycle synchronization. We found that Swe1 prematurely shifted to a partially phosphorylated form in *cdc55*Δ *cdc28-Y19F* cells (Figure 3A). Moreover, there was a loss of hypophosphorylated forms of Swe1 in *cdc55*Δ *cdc28-Y19*F cells (Figure 3A). The *cdc28-Y19F* mutant alone did not cause premature hyperphosphorylation of Swe1 (Figure 3A). In *cdc55*Δ cells, Swe1 was present in all time points due to poor cell cycle synchrony and was constitutively in the partially phosphorylated form (Figure S1A). Swe1 did not undergo premature hyperphosphorylation in *rts1*Δ cells, which indicated that $PP2A^{Rts1}$ does not play a role in opposing the initial phosphorylation of Swe1 (Figure S1B). Swe1 failed to undergo full hyperphosphorylation in *rts1*Δ cells, which suggests that $PP2A^{Rts1}$ plays a role in events required for full hyperphosphorylation of Swe1.

To further investigate the role of $PP2A^{Cdc55}$, we tested whether $PP2A^{Cdc55}$ was required for dephosphorylation of Swe1 in vivo after inhibition of an analog-sensitive allele of Cdc28 (*cdc28-as1*). We were unable to recover a *cdc28-as1 cdc55*Δ double mutant, but we were able to recover the double mutant in the presence of a kinase-dead allele of *SWE1* (*swe1-kd*) We synchronized *cdc28-as1 swe1-kd* and *cdc28-as1 swe1-kd cdc55*Δ cells and inhibited cdc28-as1 as cells were entering mitosis. Inhibition of cdc28-as1 in the control cells caused rapid and nearly complete loss of swe1-kd phosphorylation (Figure 3B). Inhibition of cdc28-as1 in *cdc55*Δ cells caused a partial dephosphorylation of swe1-kd. The partial dephosphorylation of swe1-kd could be due to another phosphatase that makes a minor contribution, or to the non-specific activity of multiple phosphatases. We further found that overexpression of Cdc55 from the *GAL1* promoter caused delayed phosphorylation of Swe1 (Figure 3C, compare 60-70 minute time points in each strain). These data, combined with the fact that *cdc55*Δ causes nearly quantitative hyperphosphorylation of Swe1 in vivo, indicate that $PP2A^{Cdc55}$ is the primary phosphatase that acts on Swe1 during early mitosis.

The *swe1-8A* mutant failed to undergo premature hyperphosphorylation in *cdc55*Δ cells, which demonstrated that $PP2A^{Cdc55}$ opposes phosphorylation of the Cdc28 consensus sites (Figure 3D). Moreover, *swe1-8A* rescued the elongated cell morphology caused by *cdc55*Δ, providing further evidence that $PP2A^{Cdc55}$ targets the consensus sites (Figure 3E, 62% of *cdc55*Δ cells were elongated, whereas no elongated cells were detected in *cdc55*Δ *swe1-8A* cells). Full hyperphosphorylation of Swe1 was delayed in *cdc55*Δ *cdc28-Y19F* cells, which indicates that $PP2A^{Cdc55}$ controls additional events required for full hyperphosphorylation of Swe1 later in mitosis (Figure 3A).

$PP2A^{Cdc55}$ can effectively oppose phosphorylation of Swe1 by Cdc28/Clb2 in vitro

To test whether $PP2A^{Cdc55}$ is likely to act directly on Swe1, we used in vitro reconstitution to test whether it can effectively oppose phosphorylation of Swe1 by Cdc28/Clb2. We used immunoaffinity chromatography with specific peptide elution to purify 3xHA-Swe1, cdc28-Y19F/Clb2-3xHA and $PP2A^{Cdc55\text{-}3xHA}$. Purifications were carried out in the

presence of 1M KCl to remove peripherally associated proteins. Examples of the purified proteins are shown in Figure S2. We used the *cdc28-Y19F* mutant to create a simplified system in which Swe1 can not phosphorylate and inhibit Cdc28, which allowed us to focus on phosphorylation of Swe1.

To ensure that reactions recapitulated conditions during early mitosis, western blotting was used to assess relative levels of Clb2 and Swe1 during the cell cycle. Clb2 and Swe1 were tagged with 3xHA at their endogenous loci in the same strain and levels of both proteins were assessed simultaneously in synchronized cells (Figure 3F). This revealed that Swe1 is present in excess during early mitosis, when Clb2 is first accumulating, and that Clb2 levels eventually exceed Swe1 levels. Note that the partially hyperphosphorylated form of Swe1 appears at low Clb2 levels in early mitosis, and that full hyperphosphorylation of Swe1 only occurs when Clb2 levels exceed Swe1 levels. Samples were electrophoresed for a short time to keep both proteins on the gel, so the resolution of Swe1 isoforms was reduced compared to Figure 3A. A similar approach revealed that Cdc55 is present in excess of both Swe1 and Clb2 (not shown).

Reactions were initiated that contained Swe1, cdc28-Y19F/Clb2, and increasing amounts of $PP2A^{Cdc55}$. The reactions were allowed to proceed for 20 minutes and phosphorylated forms of Swe1 were detected by shifts in electrophoretic mobility using an anti-HA antibody (Figure 3G). The antibody also detected Clb2-3xHA and Cdc55-3xHA, which allowed assessment of the relative amounts of each protein. Clb2-3xHA levels were just below detection, and Swe1 was present in excess of Clb2, as in early mitosis. In the absence of $PP2A^{Cdc55}$, Swe1 was quantitatively phosphorylated by cdc28-Y19F/Clb2. Added $PP2A^{Cdc55}$ effectively opposed phosphorylation of Swe1. Note that under these conditions, with very low concentrations of cdc28-Y19F/Clb2 and excess Swe1, the extensive full hyperphosphorylation of Swe1 by cdc28-Y19F/Clb2 that we previously reported was not observed (Harvey *et al.*, 2005). $PP2A^{Rts1}$ purified under identical conditions failed to oppose phosphorylation of Swe1 by Cdc28/Clb2, which suggests that Cdc55 confers specific functions upon PP2A (Figure 3G).

Inactivation of $PP2A^{Cdc55}$ causes a Swe1-dependent delay in accumulation of mitotic cyclin

We carried out in vivo experiments to further analyze the role of $PP2A^{Cdc55}$ in entry into mitosis. Previous work found that *cdc55*Δ caused a large increase in Cdc28 inhibitory phosphorylation and delayed accumulation of Clb2 (Minshull *et al.*, 1996; Yang *et al.*, 2000; Pal *et al.*, 2008). However, these studies were carried out using *cdc55*Δ cells. In contrast to the *cdc55*Δ *cdc28-Y19F* cells used for the experiments in Figure 3, *cdc55*Δ cells have significant cell cycle defects and rapidly accumulate suppressors, which makes it difficult to clearly define the immediate effects of Cdc55 inactivation. We therefore generated a temperature sensitive allele of *CDC55* (*cdc55-4*), which allowed us to determine the immediate effects of inactivating Cdc55. DNA sequencing identified a single point mutation (C875T) in the *cdc55-4* sequence compared to the wild-type *CDC55* sequence, which results in conversion of threonine 292 to methionine. Wild-type, *cdc55-4*, and *cdc55-4 swe1*Δ cells were released from a G1 arrest at the restrictive temperature and formation of mitotic spindles was assayed, as well as levels of Clb2 protein (Figures 4A and 4B). The *cdc55-4* mutant caused a prolonged delay in accumulation of Clb2 and formation of short mitotic spindles. The delay was eliminated by *swe1*Δ, which indicated that it was due to a failure to properly regulate Cdc28 inhibitory phosphorylation. The *cdc55-4* mutant caused a 10 minute delay in bud emergence, but this could not account for the 30 minute delay in formation of short mitotic spindles (Figure S3).

The *cdc55-4* mutant also caused a delay in formation of long mitotic spindles that was much greater than the delay in formation of short spindles. The delay was largely eliminated

by *swe1*Δ, which demonstrated that PP2A^{Cdc55}-dependent regulation of Cdc28 inhibitory phosphorylation also plays a role in events required for the normal timing of spindle elongation.

A potential explanation for the delay in early mitotic events is that inactivation of Cdc55 causes defects in morphogenesis that activate a Swe1-dependent checkpoint. However, previous work suggested that activation of the morphogenesis checkpoint does not cause a significant delay in accumulation of Clb2 (Carroll *et al.*, 1998). To further test this, we used a conditional septin mutant (*cdc12-6*) to activate the morphogenesis checkpoint. We detected a slight delay in accumulation of Clb2 protein in *cdc12-6* mutants; however, the delay was not comparable to the prolonged delay caused by *cdc55-4* (Figure 4C).

A threshold model for the role of PP2A^{Cdc55} in regulation of Swe1 and Cdc28

In previous work, it was hypothesized that inactivation of PP2A catalytic subunits causes reduced specific activity of Cdc28/Clb2, thereby disrupting a positive feedback loop in which Cdc28/Clb2 promotes Clb2 transcription (Amon *et al.*, 1993; Lin and Arndt, 1995). Our results provide strong support for this hypothesis: inactivation of Cdc55 caused a prolonged delay in accumulation of Clb2. Moreover, Clb2 levels rose abruptly in wild-type cells, but more gradually in *cdc55-4* cells, consistent with a failure in the positive feedback loop (Figure 4A). Our analysis of Swe1 regulation suggests an explanation for these observations. We found that Cdc28/Clb2 phosphorylates and activates Swe1, and that activation of Swe1 is opposed by PP2A^{Cdc55}. Thus, inactivation of PP2A^{Cdc55} would be expected to result in hyperactive Swe1, which would phosphorylate and inhibit Cdc28/Clb2, leading to reduced specific activity of Cdc28/Clb2 and a failure in the positive feedback loop. In this model, PP2A^{Cdc55} creates a threshold that limits activation of Swe1 by Cdc28/Clb2, thereby allowing a low level of Cdc28/Clb2 activity to accumulate in early mitosis. The low level of Cdc28/Clb2 activity triggers the positive feedback loop that promotes Clb2 transcription, without triggering full entry into mitosis. When Cdc28/Clb2 activity rises above the threshold, Swe1 would be activated to bring Cdc28/Clb2 activity back below the threshold, thus maintaining a low level of Cdc28/Clb2 activity in early mitosis. Swe1 is present in excess when mitotic cyclins first accumulate and is capable of inhibiting both nuclear and cytoplasmic pools of Cdc28 (Keaton *et al.*, 2008). Thus, a mechanism for restraining Swe1 is necessary for initiation of the positive feedback loop. Cdc55 is localized to the nucleus and the cytoplasm, so it is present where activation of Swe1 must be restrained (Gentry and Hallberg, 2002).

Swe1 is hyperactive in cells that lack PP2A^{Cdc55}

We used a combination of in vivo analysis, quantitative analysis, and mathematical modeling to test the threshold model for PP2A^{Cdc55} function. If PP2A^{Cdc55} creates a threshold that limits activation of Swe1 by Cdc28/Clb2, one would predict that Swe1 is hyperactive in cells that lack PP2A^{Cdc55}. We tested this by determining whether *cdc55*Δ cells are sensitive to increased levels of Swe1. To do this, we induced overexpression of Swe1 from the *MET25* promoter in wild-type and *cdc55*Δ cells. Expression of Swe1 in wild-type cells did not affect the rate of colony formation. In contrast, expression of Swe1 in *cdc55*Δ cells caused lethality, consistent with the idea that Swe1 is hyperactive in the absence of PP2A^{Cdc55}, leading to mitotic arrest (Figure 4D).

The phosphorylation state of Swe1 represents a steady state

We next carried out further analysis of the reconstituted system. The threshold model suggests that phosphorylation of Swe1 will approach a steady state determined by the relative activities of Cdc28/Clb2 and PP2A^{Cdc55}. In vivo analysis is consistent with this: acute inhibition of Cdc28 causes rapid dephosphorylation of Swe1, and inactivation of PP2A^{Cdc55}

causes hyperphosphorylation of Swe1 (Figure 3 and (Harvey *et al.*, 2005)). To determine whether the reconstituted system recapitulates steady state regulation of Swe1, we set up reactions containing Swe1, $PP2A^{Cdc55}$ and two different concentrations of cdc28-Y19F/Clb2. The reactions were initiated by addition of ATP and samples were taken at intervals to determine the time required to approach steady state (Figure 5A). Swe1 phosphorylation approached steady state within 10-15 minutes in the presence of both low and high levels of cdc28-Y19F/Clb2. This is a biologically relevant time scale because Clb2 accumulation in vivo occurs over a period of 40 minutes at the temperature used to carry out these reactions.

To further establish that the reactions were in dynamic opposition, a reaction was allowed to proceed for 15 minutes and okadaic acid was then added to inhibit $PP2A^{Cdc55}$. This caused rapid hyperphosphorylation of Swe1, which confirmed that phosphorylation and dephosphorylation were occurring in dynamic opposition (Figure 5B).

Quantitative analysis reveals an ultrasensitive response of Swe1 to rising levels of Cdc28/Clb2

Diverse experimental observations support the threshold model. However, a system that includes opposing kinase and phosphatase activities and multisite phosphorylation can exhibit complex behaviors, and multiple distinct behaviors are possible. To determine which of the possible behaviors is exhibited by the system, one must use quantitative analysis and fitting of experimental data to mathematical models. We therefore analyzed the reconstituted system, as well as the individual phosphorylation and dephosphorylation reactions, with the goal of determining whether the system was capable of generating the behavior postulated by the model.

We first analyzed phosphorylation of Swe1 in steady state reactions containing Swe1, $PP2A^{Cdc55}$, and increasing amounts of cdc28-Y19F/Clb2. We used fluorescent dye-based western blotting with an anti-HA antibody to detect phosphoforms of Swe1, as well as the HA-tagged Cdc55 and Clb2 added to the reactions (Figure 5C). The amounts of added Cdc28/Clb2 were set to be very low, and Swe1 levels were set to be in excess, to mimic the conditions during early mitosis. Comparison of the Clb2 signal in the in-vitro reactions with the Clb2 signal in crude extracts indicated that the amount of cdc28-Y19F/Clb2 added to the reactions was significantly lower than the peak level of Cdc28/Clb2 reached in vivo.

Four forms of Swe1 could be detected in the presence of increasing amounts of cdc28-Y19F/Clb2. These are labeled in Figure 5C as bands 1-4. Based on its electrophoretic mobility, band 4 corresponds to the form of Swe1 that is quantitatively phosphorylated on Cdc28 consensus sites. Because phosphorylation has an unpredictable effect on gel mobility, each of the lower bands may correspond to multiple forms of phosphorylated Swe1. However, the bands showed decreased electrophoretic mobility with increasing Cdc28/Clb2, indicating that they corresponded to increasingly phosphorylated forms of Swe1.

All four forms of Swe1 were quantitated in samples run in triplicate and plotted as a function of increasing amounts of cdc28-Y19F/Clb2 (Figure 5D, circles show data from three experimental replicates). Analysis of the data for three independent experiments utilizing different preparations of cdc28-Y19F/Clb2 and $PP2A^{Cdc55}$ revealed that formation of the most phosphorylated form of Swe1 (band 4) at steady state was non-linear with respect to increasing amounts of cdc28-Y19F/Clb2. This kind of non-linearity is also referred to as ultrasensitivity, which can be quantified by fitting the data to a Hill function. The corresponding Hill coefficient provides a quantitative measure of the ultrasensitivity. The Hill coefficient is sensitive to noise in the data, so we repeated the analysis using three independent preparations of purified cdc28-Y19F/Clb2 and two independent preparations of $PP2A^{Cdc55}$ and found the average Hill coefficient to be 2.56 +/- 0.43, which indicates an

ultrasensitive response (Figure 5E, each panel shows the results of an independent experiment).

We also carried out experiments to analyze phosphorylation of Swe1 as a function of increasing cdc28-Y19F/Clb2 in the absence of $PP2A^{Cdc55}$. Reactions without $PP2A^{Cdc55}$ will go to completion (i.e. complete phosphorylation of Swe1) and therefore do not represent a steady state system. Thus, we stopped the reactions after an arbitrary time to capture Swe1 in a range of intermediate phosphorylation states. We carried out three independent repetitions of the experiment using the same protein preparations used for the experiments in Figure 5E and measured Hill coefficients of 1.9, 2.0 and 2.3 (Figure S4). The fact that these reactions produced a Hill coefficient of greater than 1 suggests that there may be ultrasensitivity that is intrinsic to phosphorylation of Swe1 by Cdc28. However, these results must be treated with caution for several reasons. First, if one repeated the experiment and stopped the reactions after different amounts of time, the Swe1 dose response would look different. Therefore the ultrasensitivity of the dose response in the absence of $PP2A^{Cdc55}$ is transient and can vary over time. In particular, as time increases sufficiently for the phosphorylation reaction to go to completion, the dose response becomes constant and the Hill coefficient loses its practical meaning. Since the ultrasensitivity observed in the absence of $PP2A^{Cdc55}$ is transient, it is a different type of phenomenon and cannot be compared to that observed for steady state dose responses in the presence of $PP2A^{Cdc55}$. A related consideration is that $PP2A^{Cdc55}$ may enforce a different order of phosphorylation if it dephosphorylates sites on Swe1 with different efficiencies. In this case, phosphorylation of Swe1 in the presence or absence of $PP2A^{Cdc55}$ would represent fundamentally different reactions.

The ultrasensitive response of Swe1 to rising levels of Cdc28/Clb2 may be due to multi-step effects

Multiple mechanisms can generate ultrasensitivity, including zero-order effects, substrate competition, and multi-step effects (Goldbeter and Koshland, 1981; Gunawardena, 2005; Kim and Ferrell, 2007). Multi-step effects can arise when a kinase or phosphatase acts distributively to modify multiple sites. An enzyme that acts distributively requires more "steps" to complete the task, which leads to multi-step effects that can give rise to limited ultrasensitivity (Gunawardena, 2005). Note that distributivity says nothing about the order with which an enzyme modifies sites; a distributive enzyme may modify sites in a specific order or in a random order.

The presence of four Swe1 bands in steady state reactions indicated that at least four distinct phosphoforms of Swe1 were generated by largely distributive phosphorylation, since a completely processive mechanism would generate only two bands (i.e. unphosphorylated and fully phosphorylated Swe1). This suggested that the observed ultrasensitivity may arise predominantly from multi-step effects. To test this, we modeled the system as a phosphorylation pipeline with four stages, corresponding to the four bands in the gel, and assumed purely linear rates for phosphorylation and dephosphorylation (details provided in the Supplemental Information). To constrain the data further, we combined the steady state data in Figures 5C and 5D with data obtained by assaying the rate of phosphorylation of Swe1 by cdc28-Y19F/Clb2 in the absence of $PP2A^{Cdc55}$, and the rate of dephosphorylation of phosphorylated Swe1 by $PP2A^{Cdc55}$ in the absence of cdc28-Y19F/Clb2 activity, using the same preparations of cdc28-Y19F/Clb2 and $PP2A^{Cdc55}$ that were used for the steady state reactions shown in Figures 5C and 5D (Figures S5A and S5B, circles represent data from three replicates). We found linear rate constants that provided an excellent fit to the steady state data (represented by lines in the graphs in Figure 5D). Since we did not assume any nonlinearity in the model, which could give rise to zero-order effects or other forms of amplification, this suggests that the observed ultrasensitivity could be

accounted for entirely by multi-step effects. The data for the individual phosphorylation and dephosphorylation reactions were also fitted (Figures S5A and S5B, lines represent the behavior predicted by the model). These data were also reasonably well-reproduced by the model, although there was a slight systematic error in at least one of the graphs, which points to the limitations of describing an enzymatic system represented by 12 different graphs with a simple linear rate model involving only 6 variables. We conclude nevertheless that the model is a surprisingly accurate qualitative and quantitative representation of Swe1 phosphorylation. The linear pipeline model therefore provides a simple abstraction that largely accounts for the data, as well as a useful framework for carrying out further experiments to investigate the mechanisms underlying Swe1 phosphorylation. We emphasize that the model is not intended to provide a final or conclusive description of the mechanism of Swe1 phosphorylation. Moreover, our analysis thus far does not rule out the possibility that additional factors, such as cooperative phosphorylation of Swe1, contribute to the observed ultrasensitivity.

Interestingly, the model predicts that as the concentration of $PP2A^{Cdc55}$ is increased, the threshold value (EC50) of Cdc28/Clb2 increases proportionally (Figure S6 and Supplemental Information). With higher concentrations of $PP2A^{Cdc55}$, a higher level of active Cdc28/Clb2 is needed to counter it, which suggests that $PP2A^{Cdc55}$ can tune the level of Swe1 activation by Cdc28/Clb2.

Ultrasensitive activation of Swe1 allows generation of a stable low level of Cdc28 activity in early mitosis

How does ultrasensitivity contribute to the mechanisms that regulate Swe1 and Cdc28? In principle, the system could have evolved to generate a more simple linear response of Swe1 to increasing Cdc28/Clb2 activity. Thus, it seemed likely that the ultrasensitivity plays an important role in control of early mitotic events. We therefore used modeling to test how ultrasensitivity could affect the behavior of the system in its biological context. To do this, we followed a strategy widely adopted in engineering of "opening the loop" and considering separately the steady state response of Cdc28/Clb2 to Swe1 and the steady state response of Swe1 to Cdc28/Clb2 (details provided in the Supplemental Information). We then put the separate responses back together, thereby closing the loop, and in this way determined the system behavior.

This analysis suggested that an ultrasensitive response of Swe1 to Cdc28/Clb2 helps generate a stable level of active Cdc28/Clb2 during early mitosis, despite rising levels of Clb2. This can be seen in Figure 6A, in which we plot steady state levels of Cdc28/Clb2 activity as a function of Clb2 levels. The red lines show plots in which the final level of Cdc28/Clb2 activity was normalized to 1 to emphasize the different shapes of the curves. The blue lines show plots that were not normalized, which indicate the different levels of Cdc28/Clb2 activity that are achieved under each condition. In the absence of ultrasensitivity (n_H=1), the levels of Cdc28/Clb2 activity rise in a nearly linear manner. In contrast, an ultrasensitive response of Swe1 to Cdc28/Clb2 produces an initial rapid rise in Cdc28/Clb2 activity that then begins to level off (n_H=2.5). Thus, the ultrasensitivity may allow the system to rapidly establish and maintain a low level of Cdc28/Clb2 activity that can initiate early mitotic events, while preventing a further rise in Cdc28/Clb2 activity that would trigger full entry into mitosis.

We also carried out an analysis of the effects of varying $PP2A^{Cdc55}$ activity on the system. This showed that the level of active Cdc28/Clb2 is strongly influenced by levels of $PP2A^{Cdc55}$ activity, which provided further evidence that $PP2A^{Cdc55}$ can tune the system to control the level of Cdc28/Clb2 activity (Figure 6B). This implies that regulation of $PP2A^{Cdc55}$ could be an important mechanism for controlling levels of active Cdc28/Clb2 during early mitosis.

A quantitative model for systems-level regulation of Cdc28 and Swe1

We next generated a mechanistically-detailed mathematical model to test whether signaling interactions known to occur during mitosis are capable of generating a system that exhibits the proposed threshold behavior. We based the model on the chemical reactions described schematically in Figure 6C. Details of the model are provided in the Supplemental Information.

A sample simulation of the model is shown in Figure 6D, which is set in motion by the introduction of steadily increasing levels of Clb2. The system has several dozen variables; however, for simplicity, only three key variables are displayed in the simulation: levels of Clb2, active Cdc28/Clb2 and active Swe1. Initially, Cdc28/Clb2 is activated because active Swe1 is unavailable. After a delay in which the intermediate states of Swe1 are being formed, active Swe1 is produced, which then inactivates Cdc28/Clb2 through phosphorylation, leading to a decrease in Cdc28/Clb2 activity. At this time, a basal level of Cdc28/Clb2 activity is reached and maintained. At steady state, the Cdc28/Clb2 dimer is undergoing cycles of inhibition by Swe1 and activation by Mih1, which leads to a low basal level of Cdc28/Clb2 activity. Previous work has shown that a low basal activity of Mih1 or Cdc25 is present during interphase and early mitosis, which would allow for the reversibility of Cdc28 inhibition (Kumagai and Dunphy, 1992; Harvey *et al.*, 2005). In *Xenopus*, the low basal activity of Cdc25 is stimulated 5-fold during entry into mitosis, which is thought to help trigger full activation of Cdc28 (Kumagai and Dunphy, 1992).

Importantly, the model shows that the opposing activity of $PP2A^{Cdc55}$ can act as a threshold to generate a dynamic steady state in which a low level of Cdc28/Clb2 activity is generated and maintained in early mitosis in the presence of Swe1, despite rising Clb2 levels.

DISCUSSION

Measurement of mitotic Cdk1 activity in vertebrate cells has shown that a low plateau level of Cdk1 activity is generated in early mitosis, which is followed by switch-like full activation of Cdk1 later in mitosis (Pomerening *et al.*, 2005; Lindqvist *et al.*, 2007; Deibler and Kirschner, 2010). In budding yeast, low level activation of Cdc28 in early mitosis initiates mitotic spindle assembly, as well as a feedback loop that promotes transcription of mitotic cyclins (Amon *et al.*, 1993; Rahal and Amon, 2008). Low level activation of Cdk1 in early mitosis therefore appears to be a conserved mitotic control mechanism. A mechanism that keeps Cdk1 activity low as cyclin levels rise would allow the cell to accumulate inactive Cdk1/cyclin complexes, which could be rapidly activated via post-translational modifications to trigger full entry into mitosis. Low level activation of Cdk1 in the presence of Wee1 would also allow the cell to become poised for cell division once checkpoint conditions have been satisfied. Here, we define a systems-level mechanism by which a low level of Cdk1 activity can be generated and maintained in early mitosis, despite the presence of the Wee1 inhibitor and constantly rising cyclin levels.

Cdc28-dependent regulation of Swe1 during early mitosis

Quantitative mass spectrometry revealed that Cdc28/Clb2 phosphorylates Swe1 on a set of minimal Cdc28 consensus sites. Analysis of a *swe1-8A* mutant that lacked consensus sites showed that they are required for Swe1 activity in vivo and for formation of a Swe1-Cdc28/Clb2 complex that likely maintains Cdc28 in the inhibited state in vivo. Together, these observations suggest that phosphorylation of Cdc28 consensus sites alone drives stimulation of Swe1 activity.

Standard mass spectrometry showed that Cdc28/Clb2 phosphorylated Swe1 on non-consensus sites in addition to the consensus sites. However, these sites were phosphorylated at stoichiometries that were too low to be measured. Phosphorylation of these sites likely represents inefficient phosphorylation events that occur before Swe1 inhibits Cdc28/Clb2. The detection of these events emphasizes the high sensitivity of mass spectrometry, as well as the importance of using quantitative approaches to reveal which sites are phosphorylated at significant stoichiometries.

PP2A^{Cdc55} restrains activation of Swe1 by Cdc28

Previous studies found that inactivation of budding yeast PP2A^{Cdc55} causes increased inhibitory phosphorylation of Cdc28 and delayed mitotic progression; however, the precise roles of PP2A^{Cdc55} were unclear (Lin and Arndt, 1995; Minshull *et al.*, 1996; Yang *et al.*, 2000; Pal *et al.*, 2008). We discovered that an important function of PP2A^{Cdc55} in budding yeast is to oppose phosphorylation of Swe1 by Cdc28/Clb2. Since initial phosphorylation of Swe1 by Cdc28/Clb2 activates Swe1, we propose that PP2A^{Cdc55} sets a threshold that limits activation of Swe1 during early mitosis, thereby allowing accumulation of a low level of active Cdc28/Clb2 that can initiate the positive feedback loop that promotes transcription of mitotic cyclins (Amon *et al.*, 1993). Diverse in vivo experiments support this model. For example, inactivation of Cdc28 in vivo caused rapid dephosphorylation of Swe1 (Harvey *et al.*, 2005). Conversely, inactivation of PP2A^{Cdc55} caused premature phosphorylation of Swe1, and a mutant form of Swe1 that lacked Cdc28 consensus sites did not undergo premature phosphorylation when PP2A^{Cdc55} was inactivated. Overexpression of Cdc55 caused delayed phosphorylation of Swe1. Together, these observations demonstrate that PP2A^{Cdc55} opposes the initial activating phosphorylation of Swe1 that occurs on consensus sites. Mild overexpression of Swe1 was lethal in *cdc55*Δ cells, consistent with the idea that PP2A^{Cdc55} opposes activation of Swe1. In addition, inactivation of Cdc55 caused a prolonged delay in accumulation of Clb2, which is consistent with a failure in the positive feedback loop that promotes transcription of *CLB2*. Deletion of *SWE1* rescued the delay, which established that it was due to inappropriate inhibition of Cdc28/Clb2 by Swe1. Cells that lack PP2A^{Cdc55} may eventually enter mitosis when enough Clb2 accumulates via basal transcription to overcome the inhibitory activity of Swe1 without the help of PP2A^{Cdc55}.

In vitro reconstitution provided further support for the model. Cdc28/Clb2 was able to efficiently phosphorylate Swe1 under the conditions that prevail in early mitosis, when there are low levels of Cdc28/Clb2 and Swe1 is in excess. Moreover, purified PP2A^{Cdc55} could effectively oppose phosphorylation of Swe1 by Cdc28/Clb2. Swe1 phosphorylation in the reconstituted system approached steady state on a time scale that was relevant in vivo.

In addition to causing defects in early mitotic events, inactivation of the *cdc55-4* allele caused a prolonged delay in spindle elongation. Thus, PP2A^{Cdc55} must also control events that occur later in mitosis that are required for the normal timing of spindle elongation. The nature of the these PP2A^{Cdc55}-dependent events is unknown; however, the fact that *swe1*Δ almost completely eliminated the delay in spindle elongation indicates that PP2A^{Cdc55} exerts its effects on mitotic progression primarily via control of Cdc28 inhibitory phosphorylation. Since a high level of Cdc28 activity is required for spindle elongation, the delay may be due to delayed accumulation of active Cdc28 in the presence of hyperactive Swe1 (Rahal and Amon, 2008). Previous work found that inactivation of PP2A^{Cdc55} causes premature exit from a mitotic arrest. This phenotype is independent of Cdc28 inhibitory phosphorylation, which indicates an additional role for PP2A^{Cdc55} in late mitosis (Minshull *et al.*, 1996; Queralt *et al.*, 2006; Tang and Wang, 2006; Chiroli *et al.*, 2007).

In previous work we discovered that Mih1 is dephosphorylated during entry into mitosis by a form of PP2A^{Cdc55} that is tightly associated with a pair of redundant regulatory

subunits called Zds1 and Zds2 (Pal *et al.*, 2008; Wicky John *et al.*, 2010). The Zds1/2 proteins are not required for dephosphorylation of Swe1, which suggests they specifically target $PP2A^{Cdc55}$ to Mih1. Although the functional significance of Mih1 dephosphorylation is unclear, these results, when combined with the results reported here, indicate that $PP2A^{Cdc55}$ regulates the phosphorylation states of both Swe1 and Mih1. Importantly, *cdc55*Δ is lethal in *mih1*Δ cells and the lethality is rescued by *swe1*Δ (Pal *et al.*, 2008). Since the effects of deleting *CDC55* in *mih1*Δ cells cannot be due to misregulation of Mih1, this observation argues that $PP2A^{Cdc55}$ plays a direct role in inhibition of Swe1.

Systems-level control of Cdc28 activity during entry into mitosis

We used quantitative analysis and mathematical modeling to test the $PP2A^{Cdc55}$ threshold model and to investigate the systems-level mechanisms by which $PP2A^{Cdc55}$ controls Swe1 and Cdc28. These approaches revealed that the most phosphorylated form of Swe1 was generated in an ultrasensitive manner in response to rising levels of cdc28-Y19F/Clb2 in the reconstituted system. Systems-level modeling further suggested that the biological function of the ultrasensitivity in the system is to allow a relatively stable level of Cdc28/Clb2 activity to be rapidly generated and maintained in early mitosis despite rising Clb2 levels. The data from the reconstituted system could be fitted to a simple mathematical model in which Cdc28/Clb2 and $PP2A^{Cdc55}$ act in the linear range to move Swe1 through a series of isoforms in a phosphorylation "pipeline". The linear pipeline model provides what is perhaps the simplest abstract description of the system that could account for the data, and is intended as a guide for future investigations into the underlying mechanisms, rather than as a definitive description of the system. Although the model demonstrated that ultrasensitivity could be accounted for by multistep effects caused by multisite phosphorylation of Swe1, our results thus far do not rule out the possibility that cooperativity or other factors contribute to the observed ultrasensitivity in multisite Swe1 phosphorylation.

We also generated a mechanistically detailed systems-level model to test whether a system based on known signaling interactions in mitosis can generate the behavior postulated by the threshold model. This analysis provided an important proof of principle test of the $PP2A^{Cdc55}$ threshold model.

Quantitative analysis, modeling, and analysis of phosphorylation site mutants suggest that multisite phosphorylation of Swe1 by Cdc28/Clb2 may occur in an ordered and distributive manner. However, rigorous experimental verification of an ordered phosphorylation mechanism will require direct analysis of the phosphoforms that are produced at specific times during reactions, which may be achievable in the future via mass spectrometry. Combined experimental and mathematical analysis is an iterative process. Our analysis thus far provides a first iteration and suggests new experimental tests that will lead to a more refined understanding of the system.

Numerous studies in vertebrate cells and yeast have detected stepwise activation of Cdk1 during entry into mitosis (Pomerening *et al.*, 2005; Lindqvist *et al.*, 2007; Rahal and Amon, 2008; Deibler and Kirschner, 2010). In contrast, a recent study utilizing an in vivo biosensor detected a steady rise in mitotic Cdk1 activity in vertebrate cells (Gavet and Pines). The biosensor measured Cdk1 activity via phosphorylation of a Cdk1 consensus site in an engineered protein, which triggered a phosphorylation-dependent binding event that resulted in a FRET signal. Chemical inhibition of Cdk1 caused a slow loss of the biosensor signal over a period of 25 minutes, which indicated that the biosensor has low temporal resolution. It is unclear whether a phosphatase acts efficiently on the biosensor phosphosite, so the slow loss of the signal could be due to cyclin destruction. The low temporal resolution of the biosensor may preclude detection of dynamic Cdk1 regulation. For example, if Cdk1 phosphorylates the biosensor and is then inhibited by Wee1, the low temporal resolution of the biosensor likely means that the biosensor signal would persist long after Cdk1 is inhibited

by Wee1. Thus, the biosensor may not detect dynamic Wee1-dependent mechanisms that keep Cdk1 activity low in early mitosis.

In vertebrate cells, it has been proposed that Cdk1/cyclin A turns down Wee1 activity to allow low level activation of Cdk1/cyclin B in early mitosis (Deibler and Kirschner, 2010). In budding yeast, the Clb3 cyclin appears before Clb2 during entry into mitosis, which suggests that it could turn down Swe1 activity. If this were true, one would predict that deletion of the *CLB3* gene should cause a phenotype consistent with hyperactivity of Swe1. However, deletion of the *CLB3* gene causes no obvious phenotype (Fitch *et al.*, 1992). We therefore favor the $PP2A^{Cdc55}$ threshold model as a mechanism to restrain Swe1 activity in early mitosis. PP2A also plays a crucial role in controlling mitosis in vertebrate cells, so it could play a conserved role in restraining the activity of Wee1 family members. However, additional experiments will be necessary to test the cyclin A hypothesis and the role of PP2A in controlling Wee1 activity in vertebrates.

Phosphorylation of Wee1 has also been analyzed in *Xenopus* extracts (Kim and Ferrell, 2007). Increasing amounts of Cdk1/cyclin B1 were added to interphase egg extracts, which were incubated for 1 hour to allow the system to reach steady state. Phosphorylation of Wee1 was measured using a phosphospecific antibody that recognized a single Cdk1 consensus site. These experiments measured a Hill coefficient of 3.5 for phosphorylation of the site in crude extracts. In contrast, the Hill coefficient for phosphorylation of the site by purified cdk1-AF/cyclin B1 showed a lower Hill coefficient of 1.5. Further work suggested a model in which high concentrations of Cdk1 substrates act as competitive inhibitors in vivo to restrain phosphorylation of Wee1 by Cdk1 and to generate ultrasensitivity. An important difference between *Xenopus* egg Wee1 and Swe1 is that phosphorylation of Cdk1 consensus sites on Wee1 is thought to inactivate Wee1, although it has not yet been possible to replace endogenous *Xenopus* egg Wee1 with a phosphorylation site mutant to test this model (Kim *et al.*, 2005). The difference could be due to the presence of unique phosphorylation sites on Swe1 that function to stimulate Swe1 activity. A similar module could be present in human somatic Wee1, since it is also thought to undergo initial activation by Cdk1 (Deibler and Kirschner, 2010). Currently, it is difficult to compare regulation of Wee1 in yeast and *Xenopus* due to their evolutionary divergence and the significant technical differences in how experimental analysis has been carried out.

Theoretical analysis has shown that opposing kinase and phosphatase activities could play an important role in generating diverse and powerful signaling behaviors (Goldbeter and Koshland, 1981, 1982, 1984; Ferrell, 1996; Thomson and Gunawardena, 2009). In a number of cases, experimental analysis has provided support for this idea (LaPorte and Koshland, 1983; Nakajima *et al.*, 2005). Often, however, phosphatases are thought of as playing relatively simple roles, such as serving to reverse the activated state of a signaling pathway once the original stimulus has been removed, or to block phosphorylation of proteins to inhibit signal transduction. Analysis of the mechanisms that control Cdc28 activity in early mitosis suggests that opposing kinase and phosphatase activities are capable of generating a dynamic systems-level mechanism for modulation of signal strength. Similar mechanisms may be used to modulate signal strength in other signaling networks.

METHODS

Strains, plasmids, and culture conditions

The strains, plasmids, and culture conditions used for this study are listed in the Supplemental Information. For time course experiments, cells were grown in YPD or YPDA medium (1% yeast-extract, 2% peptone, 2% dextrose, with or without 0.004% adenine

sulfate) overnight at room temperature prior to synchronization. For induced expression experiments, cells were grown overnight in YEP medium (1% yeast extract, 2% peptone, 0.004% adenine sulfate) containing 2% glycerol/2% ethanol or 2% raffinose and then induced with 2% galactose.

Western blotting
For quantitative western blotting, proteins were transferred to Immobilon-FL (Millipore) PVDF membranes and probed with mouse monoclonal HA antibody followed by AlexaFluor 647 donkey anti-mouse secondary antibody. Blots were scanned using a Typhoon 9410 Variable Mode Imager (Amersham Biosciences) and the results were quantified with Odyssey (Licor Biosciences, v 2.1.12) and Matlab software.

Protein purifications
Immunoaffinity purifications of Cdc28/Clb2-3xHA, cdc28-Y19F/Clb2-3xHA, 3xHA-Swe1, 3xHA-swe1-8A, 3xHA-swe1-10ncs, $PP2A^{Cdc55\text{-}3xHA}$, and $PP2A^{Rts1\text{-}3xHA}$ were carried out in the presence of 1M KCl as previously described, with some modifications (Harvey *et al.*, 2005). Detailed methods for purification of proteins, including growth conditions for SILAC, are provided in the Supplemental Information.

SILAC analysis
Swe1 labeled with heavy isotope was made by expressing 3xHA-Swe1 from the *GAL1* promoter in *lys1*Δ cells in medium containing L-lysine-$^{13}C_6$,$^{15}N_2$ hydrochloride as the sole source of lysine. The protein was purified by immunoaffinity chromatography and treated with lambda phosphatase to create an unphosphorylated reference protein. The isotope labeled 3xHA-Swe1 was mixed with unphosphorylated or phosphorylated 3xHA-Swe1 and the stoichiometry of phosphorylation was determined by monitoring the depletion of unphosphorylated protein. Standard site mapping was also carried out to identify all phosphorylated sites, including those not phosphorylated at significant stoichiometries.

Co-immunoprecipitation
Association of Cdc28/3xHA-Clb2 and Swe1,swe1-8A, swe1-S133A,S263A, or swe1-T196A,T373A in crude extracts was assayed as described previously (Harvey *et al.*, 2005).

In vitro assays
See Supplemental Information for detailed reaction conditions.

Generation of Cdc55 temperature sensitive alleles
Error-prone PCR was used to generate temperature sensitive alleles of *CDC55*. DNA sequencing identified a single point mutation (C875T) in the *cdc55-4* sequence, which converts threonine 292 to methionine.

Acknowledgments
We thank David Morgan, Mart Loog, Seth Rubin, Eva Murdock, Adam Rudner, Derek McCusker, Christopher Carroll and Needhi Bhalla for critical reading of the manuscript and for helpful discussions. We thank Tracy MacDonough for help with strain construction, and the members of the laboratory for their generous support and many helpful discussions. This work was supported by a grant from the National Institutes of Health (GM069602).

References

Amon, A., Tyers, M., Futcher, B., and Nasmyth, K. (1993). Mechanisms that help the yeast cell cycle clock tick: G2 cyclins transcriptionally activate G2 cyclins and repress G1 cyclins. Cell *74*, 993-1007.

Carroll, C., Altman, R., Schieltz, D., Yates, J., and Kellogg, D.R. (1998). The septins are required for the mitosis-specific activation of the Gin4 kinase. J. Cell Biol. *143*, 709-717.

Castilho, P.V., Williams, B.C., Mochida, S., Zhao, Y., and Goldberg, M.L. (2009). The M Phase Kinase Greatwall (Gwl) Promotes Inactivation of PP2A/B55{delta}, a Phosphatase Directed Against CDK Phosphosites. Mol Biol Cell.

Chiroli, E., Rossio, V., Lucchini, G., and Piatti, S. (2007). The budding yeast PP2ACdc55 protein phosphatase prevents the onset of anaphase in response to morphogenetic defects. J Cell Biol *177*, 599-611.

Deibler, R.W., and Kirschner, M.W. (2010). Quantitative reconstitution of mitotic CDK1 activation in somatic cell extracts. Mol. Cell *37*, 753-767.

Félix, M.-A., Cohen, P., and Karsenti, E. (1990). Cdc2 H1 kinase is negatively regulated by a type 2A phosphatase in the *Xenopus* early embryonic cell cycle: evidence from the effects of okadaic acid. EMBO J. *9*, 675-683.

Ferrell, J.E., Jr. (1996). Tripping the switch fantastic: how a protein kinase cascade can convert graded inputs into switch-like outputs. Trends Biochem Sci *21*, 460-466.

Fitch, I., Dahmann, C., Surana, U., Amon, A., Nasmyth, K., Goetsch, L., Byers, B., and Futcher, B. (1992). Characterization of four B-type cyclin genes of the budding yeast *Saccharomyces cerevisiae*. Mol. Biol. Cell *3*, 805-818.

Furdui, C.M., Lew, E.D., Schlessinger, J., and Anderson, K.S. (2006). Autophosphorylation of FGFR1 kinase is mediated by a sequential and precisely ordered reaction. Mol Cell *21*, 711-717.

Gautier, J., Solomon, M.J., Booher, R.N., Bazan, J.F., and Kirschner, M.W. (1991). cdc25 is a specific tyrosine phosphatase that directly activates p34cdc2. Cell *67*, 197-211.

Gavet, O., and Pines, J. Progressive activation of CyclinB1-Cdk1 coordinates entry to mitosis. Dev Cell *18*, 533-543.

Gentry, M.S., and Hallberg, R.L. (2002). Localization of Saccharomyces cerevisiae protein phosphatase 2A subunits throughout mitotic cell cycle. Mol Biol Cell *13*, 3477-3492.

Goldbeter, A., and Koshland, D.E., Jr. (1981). An amplified sensitivity arising from covalent modification in biological systems. Proc Natl Acad Sci U S A *78*, 6840-6844.

Goldbeter, A., and Koshland, D.E., Jr. (1982). Sensitivity amplification in biochemical systems. Q Rev Biophys *15*, 555-591.

Goldbeter, A., and Koshland, D.E., Jr. (1984). Ultrasensitivity in biochemical systems controlled by covalent modification. Interplay between zero-order and multistep effects. J Biol Chem *259*, 14441-14447.

Gould, K.L., and Nurse, P. (1989). Tyrosine phosphorylation of the fission yeast cdc2^{+} protein kinase regulates entry into mitosis. Nature *342*, 39-45.

Gunawardena, J. (2005). Multisite protein phosphorylation makes a good threshold but can be a poor switch. Proc Natl Acad Sci U S A *102*, 14617-14622.

Harvey, S.L., Charlet, A., Haas, W., Gygi, S.P., and Kellogg, D.R. (2005). Cdk1-dependent regulation of the mitotic inhibitor Wee1. Cell *122*, 407-420.

Harvey, S.L., and Kellogg, D.R. (2003). Conservation of mechanisms controlling entry into mitosis: budding yeast wee1 delays entry into mitosis and is required for cell size control. Curr. Biol. *13*, 264-275.

Hoffman, I., Clarke, P.R., Marcote, M.J., Karsenti, E., and Draetta, G. (1993). Phosphorylation and activation of human cdc25-C by cdc2-cyclin B and its involvement in the self amplification of MPF at mitosis. EMBO J. *12*, 53-63.

Izumi, T., and Maller, J.L. (1993). Elimination of cdc2 phosphorylation sites in the cdc25 phosphatase blocks initiation of M-phase. Mol. Biol. Cell *12*, 1337-1350.

Izumi, T., and Maller, J.L. (1995). Phosphorylation and activation of the Xenopus Cdc25 phosphatase in the absence of Cdc2 and Cdk2 kinase activity. Mol. Biol. Cell *6*, 215-216.

Izumi, T., Walker, D.H., and Maller, J.L. (1992). Periodic changes in the phosphorylation of the Xenopus Cdc25 phosphatase regulate its activity. Mol. Biol. Cell *3*, 927-939.

Jorgensen, P., Nishikawa, J.L., Breitkreutz, B.J., and Tyers, M. (2002). Systematic identification of pathways that couple cell growth and division in yeast. Science *297*, 395-400.

Karlsson-Rosenthal, C., and Millar, J.B. (2006). Cdc25: mechanisms of checkpoint inhibition and recovery. Trends Cell Biol *16*, 285-292.

Keaton, M.A., and Lew, D.J. (2006). Eavesdropping on the cytoskeleton: progress and controversy in the yeast morphogenesis checkpoint. Curr Opin Microbiol *9*, 540-546.

Keaton, M.A., Szkotnicki, L., Marquitz, A.R., Harrison, J., Zyla, T.R., and Lew, D.J. (2008). Nucleocytoplasmic Trafficking of G2/M Regulators in Yeast. Mol Biol Cell.

Kellogg, D.R. (2003). Wee1-dependent mechanisms required for coordination of cell growth and cell division. J Cell Sci *116*, 4883-4890.

Kim, S.Y., and Ferrell, J.E., Jr. (2007). Substrate competition as a source of ultrasensitivity in the inactivation of Wee1. Cell *128*, 1133-1145.

Kim, S.Y., Song, E.J., Lee, K.J., and Ferrell, J.E., Jr. (2005). Multisite M-phase

phosphorylation of Xenopus Wee1A. Mol Cell Biol *25*, 10580-10590.

Kumagai, A., and Dunphy, W.G. (1991). The cdc25 protein controls tyrosine dephosphorylation of the cdc2 protein in a cell-free system. Cell *64*, 903-914.

Kumagai, A., and Dunphy, W.G. (1992). Regulation of the cdc25 protein during the cell cycle in Xenopus extracts. Cell *70*, 139-151.

LaPorte, D.C., and Koshland, D.E., Jr. (1983). Phosphorylation of isocitrate dehydrogenase as a demonstration of enhanced sensitivity in covalent regulation. Nature *305*, 286-290.

Lin, F.C., and Arndt, K.T. (1995). The role of *Saccharomyces cerevisiae* type 2A phosphatase in the actin cytoskeleton and in entry into mitosis. EMBO J. *14*, 2745-2759.

Lindqvist, A., van Zon, W., Karlsson Rosenthal, C., and Wolthuis, R.M. (2007). Cyclin B1-Cdk1 activation continues after centrosome separation to control mitotic progression. PLoS Biol *5*, e123.

Minshull, J., Straight, A., Rudner, A.D., Dernburg, A.F., Belmont, A., and Murray, A.W. (1996). Protein phosphatase 2A regulates MPF activity and sister chromatid cohesion in budding yeast. Curr. Biol. *6*, 1609-1620.

Mochida, S., Ikeo, S., Gannon, J., and Hunt, T. (2009). Regulated activity of PP2A-B55 delta is crucial for controlling entry into and exit from mitosis in Xenopus egg extracts. EMBO J *28*, 2777-2785.

Morgan, D.O. (2007). The Cell Cycle: Principles of Control. Oxford University Press.

Mueller, P.R., Coleman, T.R., and Dunphy, W.G. (1995). Cell cycle regulation of a Xenopus Wee1-like kinase. Mol Biol Cell *6*, 119-134.

Nakajima, M., Imai, K., Ito, H., Nishiwaki, T., Murayama, Y., Iwasaki, H., Oyama, T., and Kondo, T. (2005). Reconstitution of circadian oscillation of cyanobacterial KaiC phosphorylation in vitro. Science *308*, 414-415.

Nash, P., Tang, X., Orlicky, S., Chen, Q., Gertler, F.B., Mendenhall, M.D., Sicheri, F., Pawson, T., and Tyers, M. (2001). Multisite phosphorylation of a CDK inhibitor sets a threshold for the onset of DNA replication. Nature *414*, 514-521.

Nurse, P. (1975). Genetic control of cell size at cell division in yeast. Nature *256*, 547-551.

Ong, S.E., Blagoev, B., Kratchmarova, I., Kristensen, D.B., Steen, H., Pandey, A., and Mann, M. (2002). Stable isotope labeling by amino acids in cell culture, SILAC, as a simple and accurate approach to expression proteomics. Mol Cell Proteomics *1*, 376-386.

Pal, G., Paraz, M.T., and Kellogg, D.R. (2008). Regulation of Mih1/Cdc25 by protein phosphatase 2A and casein kinase 1. J Cell Biol *180*, 931-945.

Pomerening, J.R., Kim, S.Y., and Ferrell, J.E., Jr. (2005). Systems-level dissection of the cell-cycle oscillator: bypassing positive feedback produces damped oscillations. Cell *122*, 565-578.

Queralt, E., Lehane, C., Novak, B., and Uhlmann, F. (2006). Downregulation of PP2A(Cdc55) phosphatase by separase initiates mitotic exit in budding yeast. Cell *125*, 719-732.

Rahal, R., and Amon, A. (2008). Mitotic CDKs control the metaphase-anaphase transition and trigger spindle elongation. Genes Dev *22*, 1534-1548.

Rupes, I. (2002). Checking cell size in yeast. Trends Genet. *18*, 479-485.

Russell, P., and Nurse, P. (1986). cdc25+ functions as an inducer in the mitotic control of fission yeast. Cell *45*, 145-153.

Russell, P., and Nurse, P. (1987). Negative regulation of mitosis by wee1+, a gene encoding a protein kinase homolog. Cell *49*, 559-567.

Solomon, M.J., Glotzer, M., Lee, T.H., Philippe, M., and Kirschner, M.W. (1990). Cyclin activation of $p34^{cdc2}$. Cell *63*, 1013-1024.

Sreenivasan, A., and Kellogg, D. (1999). The Elm1 kinase functions in a mitotic signaling network in budding yeast. Mol. Cell. Biol. *19*, 7983-7994.

Tang, X., and Wang, Y. (2006). Pds1/Esp1-dependent and -independent sister chromatid separation in mutants defective for protein phosphatase 2A. Proc Natl Acad Sci U S A *103*, 16290-16295.

Tang, Z., Coleman, T.R., and Dunphy, W.G. (1993). Two distinct mechanisms for negative regulation of the Wee1 protein kinase. Embo J *12*, 3427-3436.

Theesfeld, C.L., Irazoqui, J.E., Bloom, K., and Lew, D.J. (1999). The role of actin in spindle orientation changes during the Saccharomyces cerevisiae cell cycle. J Cell Biol *146*, 1019-1032.

Thomson, M., and Gunawardena, J. (2009). Unlimited multistability in multisite phosphorylation systems. Nature *460*, 274-277.

Wicky John, S., Tjandra, H., Schieltz, D., Yates III, J., and Kellogg, D.R. (2010). The Zds proteins control entry into mitosis and target protein phosphatase 2A to the Cdc25 phosphatase. Mol Biol Cell *22,* 20-32*.*

Yang, H., Jiang, W., Gentry, M., and Hallberg, R.L. (2000). Loss of a protein phosphatase 2A regulatory subunit (Cdc55p) elicits improper regulation of Swe1p degradation. Mol Cell Biol *20*, 8143-8156.

Table 1. Estimated fractional phosphorylation occupancy of key sites in Swe1. For peptides with multiple phosphorylation sites, the fractional occupancy indicates the fraction of peptides phosphorylated on one or more sites; the fractional occupancy of individual sites could not be determined. Swe1 was purified from yeast grown in the presence of ^{13}C stably isotopically labeled lysine ("heavy") or natural lysine ("light") and phosphatase treated. Light Swe1 was incubated in a mock reaction without added kinase or with Cdk1/Clb2. The light Swe1 from each reaction was then mixed with heavy Swe1 that had been treated with phosphatase and the mixtures were resolved by SDS-PAGE. Coomassie blue-stained bands were excised, proteolysed, and examined by LC-MS/MS on an LTQ-Orbitrap mass spectrometer, and matched to peptide sequences using SEQUEST. Heavy:Light abundance ratios of unphosphorylated peptides were automatically calculated using Vista. As peptides become phosphorylated, the pool of light unphosphorylated peptides is depleted and the H:L ratio increases. Using ratios for peptides that lack serine, threonine, and tyrosine as a baseline, we calculated the phosphorylated fraction for each peptide as $F_{Phos} = 1- F_{Un}/F_{Pep}$ where F_{Phos} = fraction phosphorylated, F_{Un} = average H:L ratio of unphosphorylatable peptides in each experiment, and F_{Pep} = average H:L ratio of each unphosphorylated peptide. Phosphorylation sites for each peptide were inferred from the appearance of peptides bearing these sites in the light fraction upon phosphorylation with Cdk1/Clb2. Confidently localized sites are shown bolded and underlined. Where we were unable to determine precise site localization brackets indicate the range of possible assignments. LysC digested and trypsin digested samples represent distinct biological replicates of the experiments. ND - not determined.

		Fractional Occupancy	
Site	**Local Sequence**	**LysC**	**Trypsin**
T45	IGGS**T**PTNK	86%	88%
S111, T121[1]	IKRW**S**PFHENESVT**T**PITK	95%	94%
S133	EKTN**S**PISL	97%	97%
[159-162]	TSSS[SSYS]VAK	55%	62%
T196	RIPE**T**PVKK	98%	99%
S201	PVKK**S**PLVE	49%	ND
S263	TIDS**S**PLSE	97%	97%
T280, S284, [286-297][1]	HNNQ**T**NIL**S**P[TNSLVTNSSPQT]LHSN	96%	97%
T373	EEIS**T**PTRR	96%	ND
S418	TDSS**S**PLNSK	ND	94%

[1] The stoichiometry of these sites could not be assessed independently. Reported data indicate the fraction of peptides phosphorylated on one or more sites.

FIGURE LEGENDS

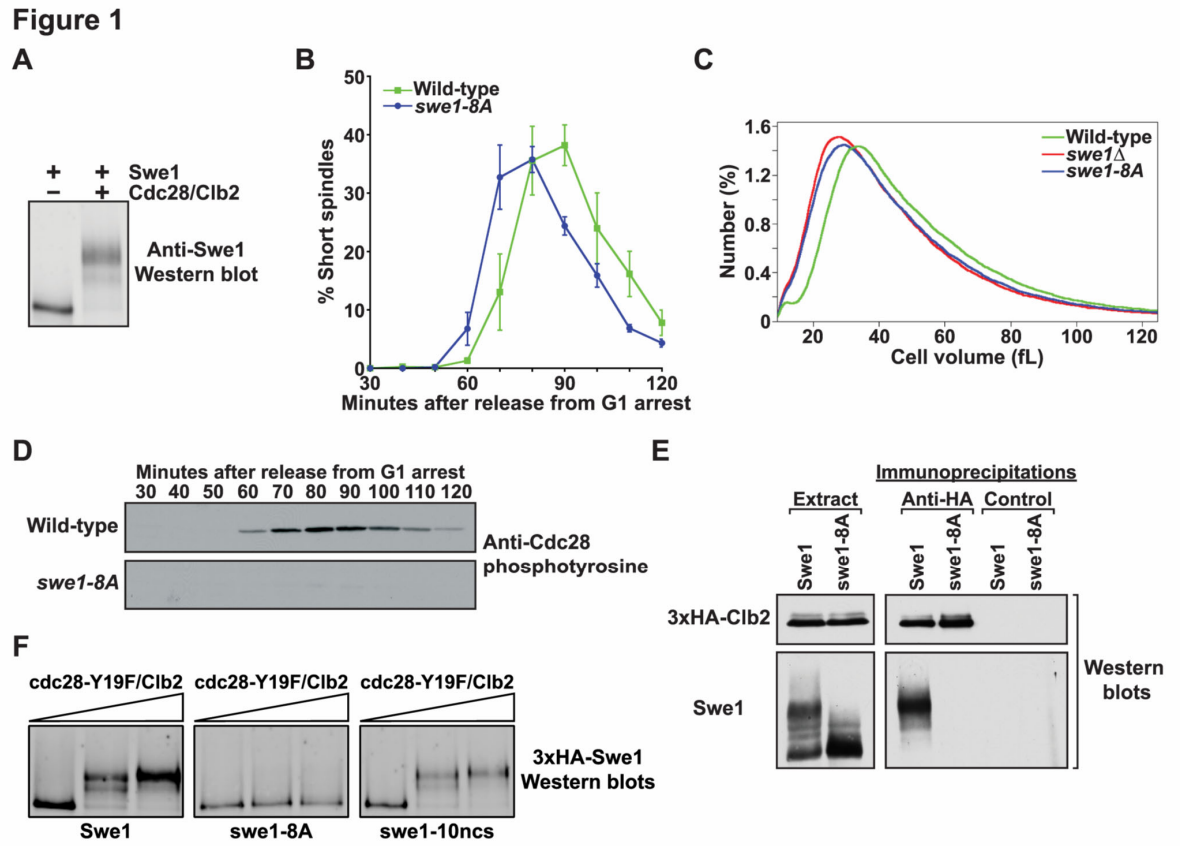

Figure 1. Phosphorylation of Cdc28 consensus sites is necessary for Swe1 activity in vivo. (A) Purified Cdc28/Clb2 quantitatively phosphorylates purified Swe1 in vitro. Phosphorylation of Swe1 causes an electrophoretic mobility shift that is detected by a western blot. (B) Wild-type and *swe1-8A* cells were released from a G1 arrest and the percentage of cells with short mitotic spindles was determined at the indicated times and plotted as a function of time. Error bars represent SEM for three independent experiments. (C) Cell size distributions of log phase cultures of wild-type, *swe1*Δ, and *swe1-8A* strains. Each trace is the average of 15 independent cultures. (D) Cells of the indicated genotypes were released from a G1 arrest and samples were taken at the indicated times. Cdc28 phosphotyrosine was monitored by western blot. (E) Wild-type and *swe1-8A* cells carrying *GAL1-3xHA-CLB2* were grown to mid-log phase and expression of 3xHA-Clb2 was induced with 2% galactose for 3 hours at 30°C. Extracts were made and 3xHA-Clb2 was immunoprecipitated with an anti-HA antibody. As a control, identical precipitations were carried out using an anti-GST antibody. Co-precipitation of Swe1 was assayed by western blot. The panels labeled "Extract" show western blots of 3xHA-Clb2 and Swe1 in the crude extracts used for the immunoprecipitations. (F) Purified 3xHA-Swe1, 3xHA-swe1-8A, or 3xHA-swe1-10ncs were incubated with increasing amounts of purified cdc28-Y19F/Clb2-3xHA in the presence of ATP. Phosphorylation of Swe1 was detected as an electrophoretic mobility shift on a western blot.

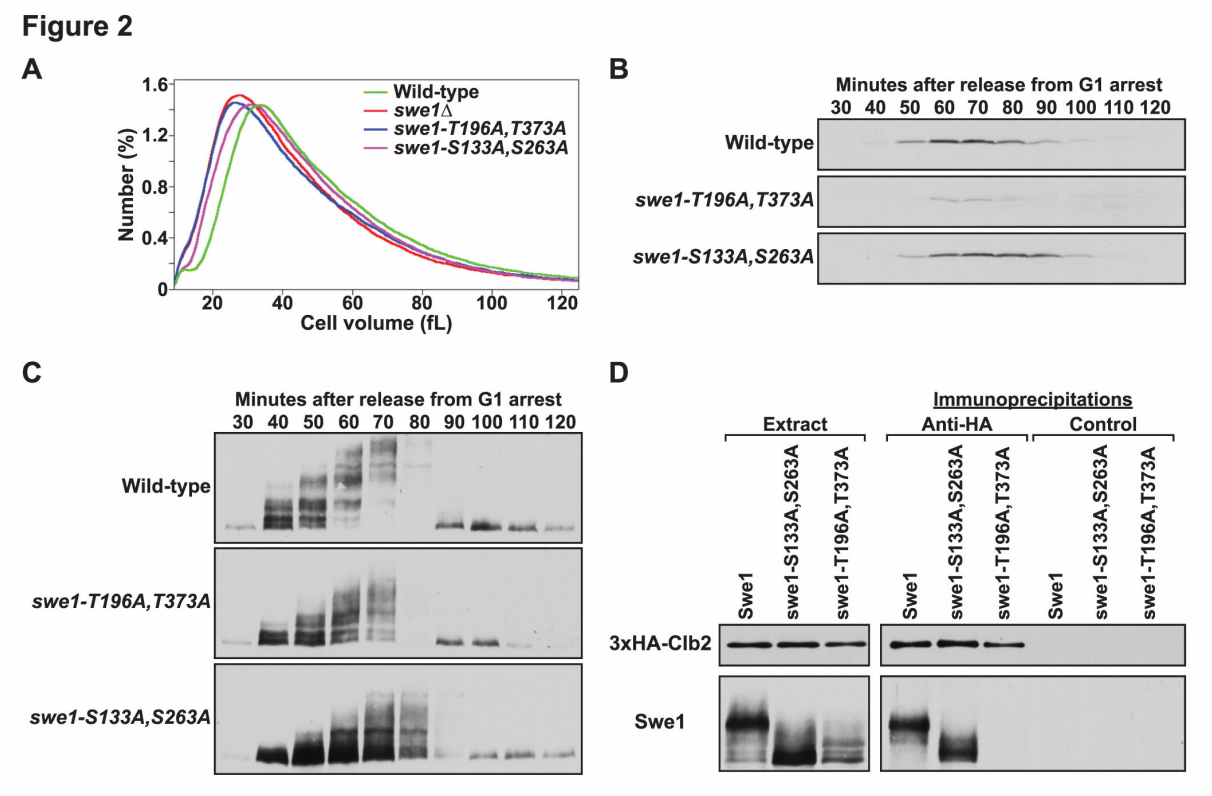

Figure 2. Analysis of Swe1 phosphorylation site mutants. (A) Cell size distributions of log phase cultures of wild-type, *swe1*Δ, *swe1-T196A,T373A*, and *swe1-S133A,S263A*. Each trace is the average of 15 independent cultures. The wild-type and *swe1*Δ traces plotted in Figure 1C and panel A are identical. (B and C) Cells of the indicated genotypes were released from a G1 arrest into 30°C YPDA medium and samples were taken at the indicated times. The behavior of (B) Cdc28 phosphotyrosine and (C) Swe1 was assayed by western blot. **(D) Wild-type, *swe1-S133A,S263A,* and *swe1-T196A,T373A* cells carrying *GAL1-3xHA-CLB2* were grown to mid-log phase and expression of 3xHA-Clb2 was induced with 2% galactose for 3 hours at 30°C. Extracts were made and 3xHA-Clb2 was immunoprecipitated with an anti-HA antibody. As a control, identical precipitations were carried out using an anti-GST antibody. Co-precipitation of Swe1 was assayed by western blot.**

Figure 3

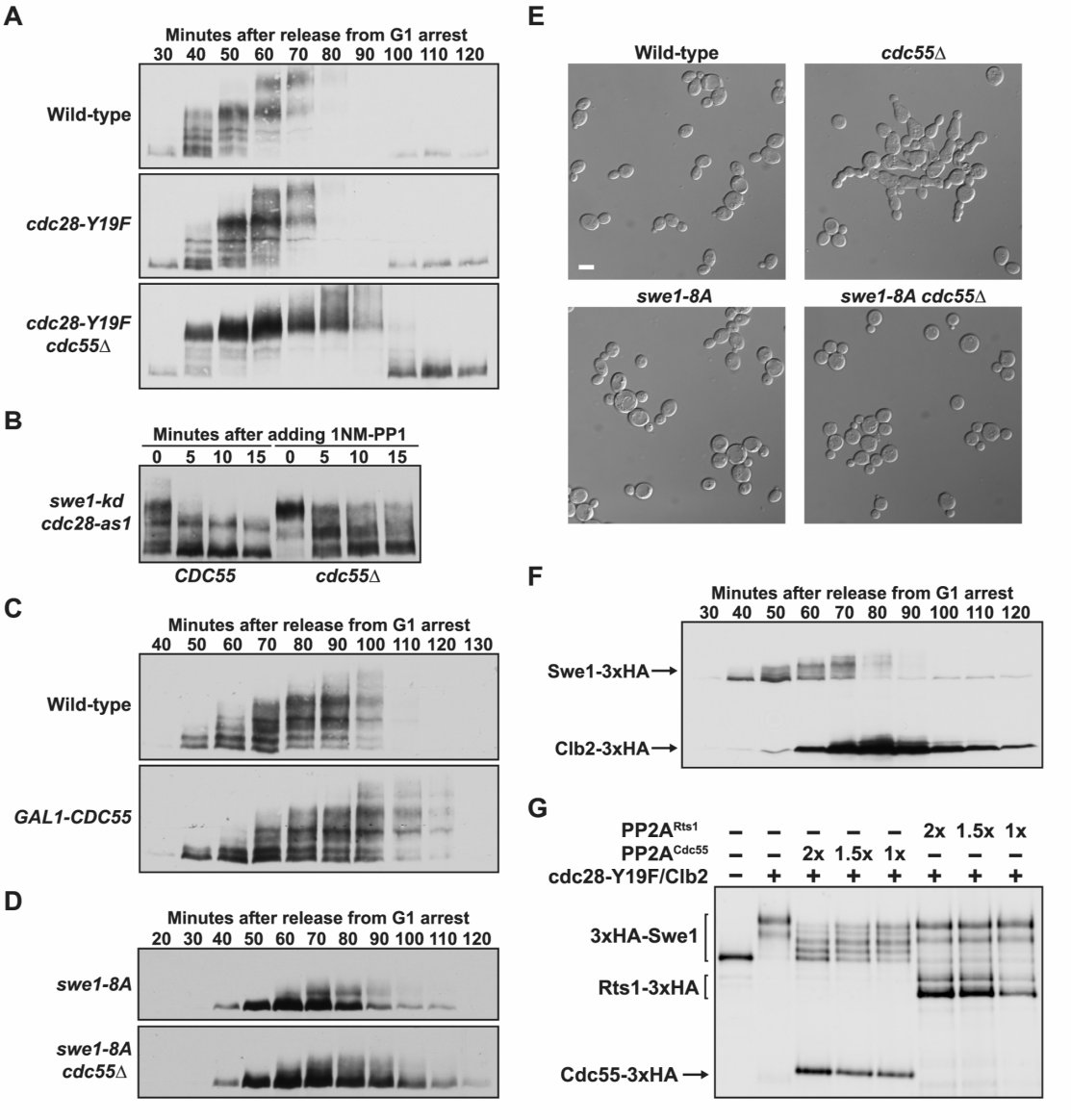

Figure 3. PP2A^{Cdc55} opposes the initial phosphorylation of Swe1 by Cdc28. (A) Cells of the indicated genotypes were released from a G1 arrest and the behavior of Swe1 was assayed by western blot. The strains used for this experiment were generated in the A364A background. Similar results were obtained in the W303-1A strain background. (B) 1NM-PP1 was added to *cdc28-as1 swe1-kd* or *cdc28-as1 swe1-kd cdc55*Δ cells 65 minutes after release from a G1 arrest. Swe1 phosphorylation was assayed by western blot. (C) Cells were grown overnight in YEP medium containing 2% raffinose and then arrested with alpha factor at room temperature. After a 2 hour incubation in the presence of alpha factor, 2% galactose was added to initiate expression of *GAL1-CDC55* and the incubation was continued for an additional 1 hour. Cells were released from the arrest into galactose-containing YEP medium and the behavior of Swe1 was assayed by western blot. (D) Cells of the indicated genotypes were released from a G1 arrest into 30°C YPD medium and the behavior of Swe1 was assayed by western blot. (E) Cells of the indicated genotypes were grown overnight to log phase at room temperature in YPD medium and imaged by differential

interference contrast microscopy. Scale bar: 5 μm. (F) Cells carrying Clb2-3xHA and Swe1-3xHA were released from a G1 arrest into 30°C YPD medium and the behavior of Clb2 and Swe1 was monitored on the same western blot. (G) The indicated combinations of purified protein complexes were incubated in the presence of ATP and purified dephosphorylated Swe1 for 20 minutes and then analyzed by western blot. All of the 3xHA-tagged proteins were detected on the same blot with an anti-HA antibody. Three different concentrations of $PP2A^{Cdc55}$ or $PP2A^{Rts1}$ were added to the reactions that varied over a 2-fold range, which are indicated as 1X, 1.5X and 2X.

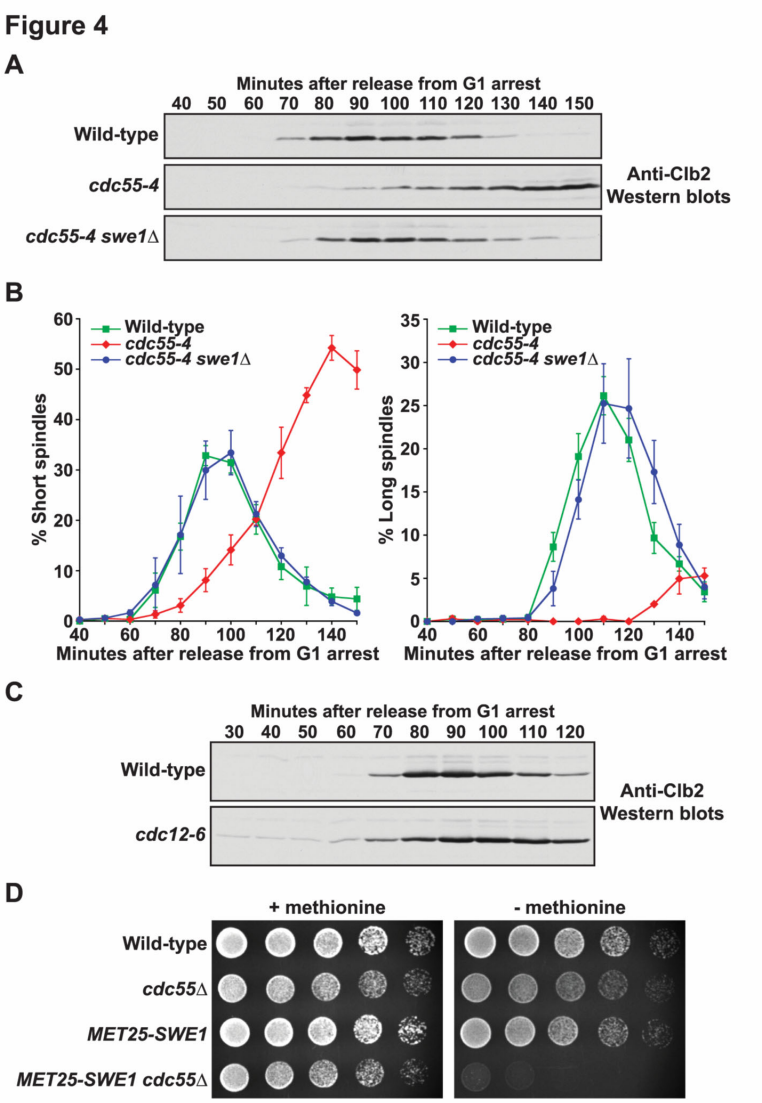

Figure 4. Inactivation of PP2A^{Cdc55} causes a Swe1-dependent delay in Clb2 accumulation. (A and B) Cells of the indicated genotypes were released from a G1 arrest into 35°C YPD medium. Samples were taken every 10 minutes at the indicated times. (A) Clb2 protein levels were monitored by western blot. (B) The percentage of cells with short or long spindles was determined and plotted as a function of time. Error bars represent SEM for three independent experiments. (C) Cells of the indicated genotypes were grown overnight to log phase and then arrested with alpha factor for 4 hours at 20°C. Cells were released from the G1 arrest into 37°C YPD medium. Samples were taken every 10 minutes at the indicated times and Clb2 protein levels were monitored by western blot. (D) 5-fold serial dilutions of cells of the indicated genotypes were grown on minimal media plates containing 2% dextrose in the presence or absence of 20 μg/ml L-methionine at 30°C. The *MET25* promoter is induced in the absence of L-methionine.

Figure 5

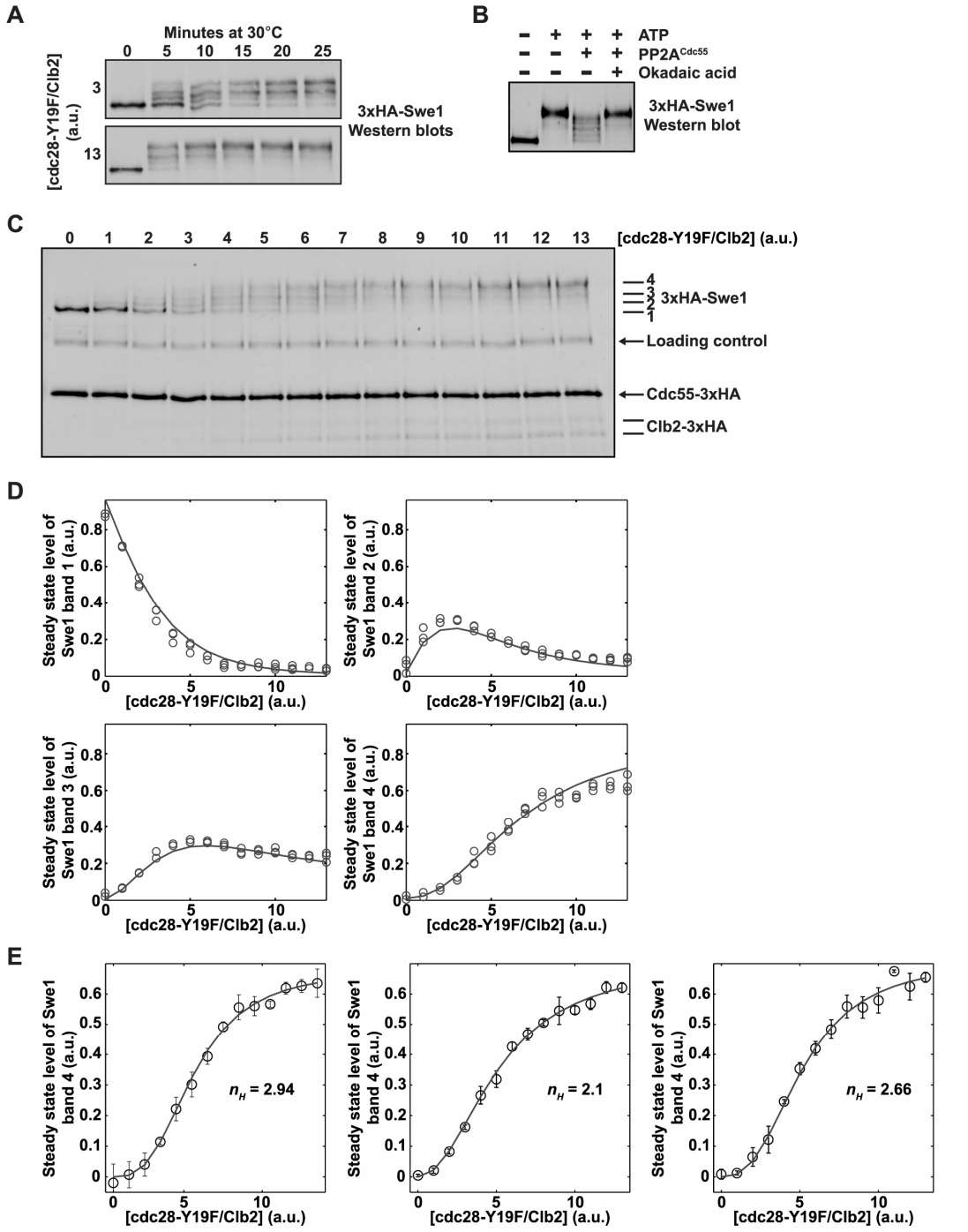

Figure 5. The response of Swe1 to rising levels of cdc28-Y19F/Clb2 is ultrasensitive. (A) Reactions containing Swe1, PP2A^{Cdc55}, and two concentrations of cdc28-Y19F/Clb2 were initiated by addition of ATP. Samples were taken at the indicated times and the phosphorylation state of Swe1 was assayed by western blot. The amounts of cdc28-Y19F/Clb2 were chosen to demonstrate that the reactions carried out in panel C approach steady state within the reaction time at both low and high concentrations of cdc28-Y19F/Clb2

(a.u., arbitrary units). (B) Reactions containing Swe1 and cdc28-Y19F/Clb2 were incubated for 15 minutes in the presence or absence of ATP and $PP2A^{Cdc55}$ (lanes 1-3). Samples were taken from each reaction and okadaic acid was then added to the reaction in lane 3, which was incubated for an additional 10 minutes before taking a sample (lane 4). Swe1 phosphorylation was assayed by western blot. (C) Phosphorylation of Swe1 (bands labeled 1-4) as a function of cdc28-Y19F/Clb2 concentration in the presence of a constant amount of $PP2A^{Cdc55}$. Reactions were allowed to proceed for 20 minutes. AlexaFluor 647-labeled phosphorylase B was used as a loading control. Proteins were assayed by quantitative western blotting using a monoclonal HA antibody to detect each 3xHA-tagged protein. (D) Quantitation of the amount of each Swe1 band generated in the reactions shown in panel C. Reactions were analyzed in triplicate; circles represent data from each of the three replicates. Each graph also shows a line that represents the solution of the pipeline model described in the Supplemental Information. (E) Swe1 shows an ultrasensitive response to rising levels of cdc28-Y19F/Clb2. We repeated the analysis using three independent preparations of purified cdc28-Y19F/Clb2 and two independent preparations of $PP2A^{Cdc55}$ to create three biological replicates of the steady state analysis, and each biological replicate was measured in triplicate. The graphs show the average quantitation of the amount of Swe1 band 4 generated as a function of cdc28-Y19F/Clb2 concentration for each biological replicate. Error bars represent standard deviation. In each graph, a Hill function was fit through least squares approximation, and the Hill coefficients (n_H) are displayed.

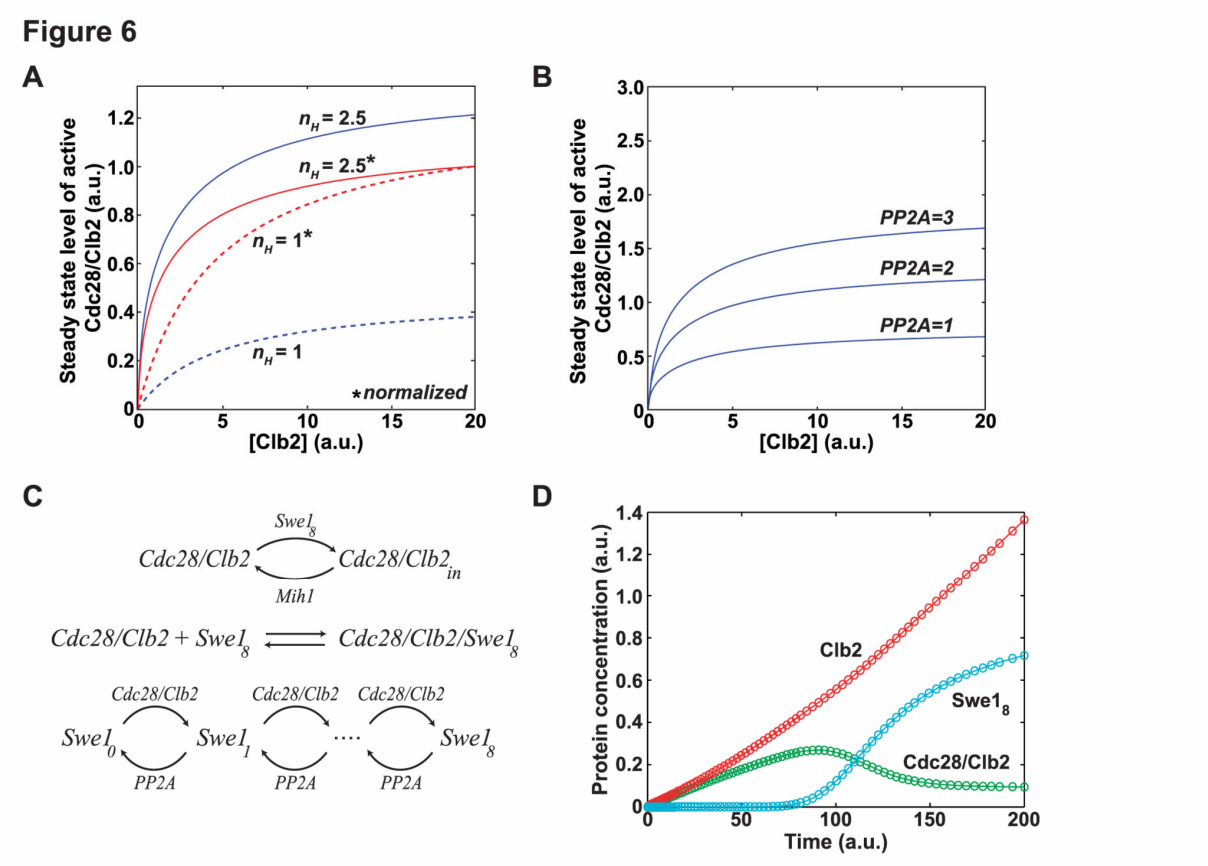

Figure 6. Systems-level regulation of Cdc28 and Swe1 by PP2A^{Cdc55} in early mitosis. (A) The steady state activity of Cdc28/Clb2 was calculated by intersecting the dose response curves in Figures S7A and S7B and the resulting values were plotted for different Clb2 concentrations. The solid and dotted lines were determined using the solid and dotted lines in Figure S7A (see Supplemental Information for details, including parameter values) (a.u., arbitrary units). The red lines show plots in which the final level of Cdc28/Clb2 activity was normalized to 1 to emphasize the different shapes of the curves. The blue lines show plots that were not normalized, which indicate the different levels of Cdc28/Clb2 activity that are achieved under each condition. (B) Using the response curve for n_H=2.5 in Figure 6A, the same graph as in panel A is plotted for increasing PP2A^{Cdc55} concentrations. (C and D) A detailed quantitative model of the interactions between Swe1, Clb2, Cdc28, and PP2A^{Cdc55} during entry into mitosis. (C) The chemical reactions which define the network, using mass action terms for each interaction. (D) A sample time course of the model, set in motion by a steadily increasing Clb2 concentration. The red line shows rising Clb2 levels, the green line shows Cdc28/Clb2 activity, and the blue line shows Swe1 activity.

Mathematical Analysis of Swe1 Phosphorylation

The dynamics of Swe1 phosphorylation can be described by a linear pipeline model

In this section we discuss in detail the simple pipeline model used to describe the phosphorylation and dephosphorylation dynamics of Swe1. As mentioned in the main text, we classify Swe1 protein into forms depending on their position on the western blot. We label their concentration as S_1 through S_4 from the bottom to the top of the gel. Therefore one would expect S_1 to contain the least phosphorylated phosphoform(s), and so on. Only S_4, the most phosphorylated band, is assumed to be active as a kinase towards Cdk1. Similar models were described in (Serber and Ferrell, 2007) and (Furdui et al, 2006), the latter of which also produced strong experimental evidence for this type of sequential phosphorylation.

The kinase acting on Swe1 is the active (unphosphorylated) version of the Cdk1/Clb2 dimer, or to be more precise in this case, the constitutively active dimer cdk1-Y19F/Clb2. We represent the concentration of this dimer by the variable C. We also denote the concentration of the phosphatase, PP2A^{Cdc55}, by the variable P. We assume that the transition rate from each band S_i to S_{i+1} is proportional to CS_i, and that the transition rate from S_i to S_{i-1} is proportional to PS_i. The model then has the form

$$\begin{aligned}
\frac{d}{dt}S_1 &= -a_1 C\cdot S_1 + b_1 P\cdot S_2 \\
\frac{d}{dt}S_2 &= a_1 C\cdot S_1 - b_1 P\cdot S_2 - a_2 C\cdot S_2 + b_2 P\cdot S_3 \\
\frac{d}{dt}S_3 &= a_2 C\cdot S_2 - b_2 P\cdot S_3 - a_3 C\cdot S_3 + b_3 P\cdot S_4 \\
\frac{d}{dt}S_4 &= a_3 C\cdot S_3 - b_3 P\cdot S_4 .
\end{aligned} \tag{1}$$

We have written in Table A the names of the different proteins involved here and below. This model was used to fit the data in Figure 4, as well as the additional experiments in Figure S3, using a single set of parameter values found through least squares error approximation ($a = 10^{-2}(4, 6.7, 2.2), b = 10^{-2}(10.6, 14.5, 5.3)$).

Notice that this model is linear for given fixed values of P and C. It is easy to see that the sum of all forms of Swe1 remains constant over time, i.e. $S_1 + S_2 + S_3 + S_4 = S_{tot}$. Also, at steady state we have the following equations:

$$a_1 CS_1 = b_1 PS_2,\ a_2 CS_2 = b_2 PS_3,\ a_3 CS_3 = b_3 PS_4. \tag{2}$$

$S_1 \ldots S_4$	Swe1 in various levels of phosphorylation
C	active Cdk1/Clb2, also cdk1-Y19F/Clb2
P	PP2A^{Cdc55}
D	total Cdk1/Clb2 (both active and inactive)
L	Clb2 monomer
M	Mih1

Table A: A list of the notations used for proteins in (1) and (5).

From here one can solve for S_4 to obtain

$$S_4 = S_{tot} \frac{\frac{a_1 a_2 a_3}{b_1 b_2 b_3}\left(\frac{C}{P}\right)^3}{1+\frac{a_1}{b_1}\frac{C}{P}+\frac{a_1 a_2}{b_1 b_2}\left(\frac{C}{P}\right)^2+\frac{a_1 a_2 a_3}{b_1 b_2 b_3}\left(\frac{C}{P}\right)^3}. \qquad (3)$$

For concreteness, we assign to the parameters the values $a_1 / b_1 = a_2 / b_2 = a_3 / b_3 = 1, S_{tot} = 6$. See (Gunawardena, 2005), where a more detailed model of multisite phosphorylation implies the same formula for the steady state of the most phosphorylated protein. We will consider this expression as a function of C, while leaving all other variables fixed, and denote it by $S_4 = f(C)$. This formula shows how multiple linear phosphorylation steps can result in a nonlinear, sigmoidal response.

Notice that as the fixed phosphatase concentration increases, it shifts the threshold of the function of C to the right. To be precise, let us call $K_{D,f}$ the threshold constant for f, i.e. the concentration of C for which $f(C)$ is half its maximum value. If the concentration P is doubled, then C will need to be twice as large for S_4 to reach its previous steady state level, since C is divided by P in (3). Therefore the new threshold $K_{D,f}$ must be twice as large as the old threshold (see Figure S4). In general, $K_{D,f}$ is proportional to P and it can be effectively tuned by changing this concentration.

When applying this model to the data in Figure 4C, we should address the processivity of this biological system. A modifying enzyme is said to act in a *distributive* manner if it makes at most one modification (addition or removal of a phosphate) at a time; it is *processive* if it makes more than one. Because of the unpredictable effect of phosphorylation on gel mobility, we cannot know for certain how many phosphoforms are actually present in any given gel band, but the existence of the four bands suggests that, if there is any processivity, it has only a moderate impact.

A systems-level decomposition of in vivo Swe1 and Cdk1 phosphorylation

We next describe the dynamics between Swe1 and Cdk1, with a focus on understanding the role of the ultrasensitive response of Swe1 in (1) and the control by PP2A^{Cdc55}. We expand on the equations in (1) by including a rate equation for Cdk1/Clb2 itself. The dynamics of Cdk1/Clb2 is tied to other variables such as the phosphatase Mih1, hence we write a general system of differential equations in the form

$$\frac{d}{dt}(C, Cdk1, Clb2, \ldots) = H(C, Cdk1, Clb2, \ldots; S_4). \qquad (4)$$

Notice that S_4 is included in the right hand side of this system, as a kinase for Cdk1/Clb2. We continue to refer by the label C the concentration of the active Cdk1/Clb2 dimer, although now we are referring to the wild-type protein instead of cdk1-Y19F.

The two coupled systems of equations (1) and (4) together form a basic model of the interactions between Swe1 and Cdk1. However, an interesting approach is to consider (1) and (4) separately, using C as a constant parameter in system (1), S_4 also as a parameter in (4). The former case was actually carried out in the first section, simply by letting C stand for cdk1-Y19F/Clb2, i.e. a protein that cannot itself be affected by Swe1. This leaves the action of Cdk1 on Swe1 unchanged, but the concentration of C itself remains essentially constant.

In order to isolate (4) into an uncoupled system, one could use a constitutively active form of Swe1 which cannot be further affected by Cdk1, or simply set the concentration of PP2A^{Cdc55} to zero and use fully phosphorylated Swe1 - this way the concentration of active Swe1 stays constant regardless of the value of C.

For every fixed concentration C in the uncoupled system of equations (1), we let system (1) converge towards steady state and define $f(C)$ to be the concentration of S_4 in this steady state - see Figure S51. Similarly, for every fixed concentration S_4 in the open loop system (4), we let the system converge to equilibrium (assuming it does so), and call $g(S_4)$ the steady state concentration of C. Notice that while $f(C)$ is increasing as a function of C, it is to be expected that $g(S_4)$ is decreasing as a function of S_4 (Figure S52). This is because S_4 has the role of inhibiting C by phosphorylation. Moreover, the function $g(S_4)$ should also depend on the concentration of Clb2, which we assume to increase slowly enough that it can be treated as a constant over a shorter timescale.

We further specify the function $g(S_4)$ as follows. For a given concentration L of Clb2, we suppose that there is a steady state concentration of total dimer Cdk1/Clb2 (that is, where Cdk1 can be both active or inactive). We denote this concentration by D and describe the dependence on L as $D = r_1 L/(r_2 + L)$. We define $g(S_4)$ to have the general form $g(S_4) = V_{\max,g} \dfrac{EC50_g^m}{EC50_g^m + S_4^m}$, where the ultrasensitive behavior of C to S_4 is assumed due to sources such as positive feedback interactions with Mih1. We set $V_{\max,g} = g(0) = D$, since presumably when $S_4 = 0$ all the Cdk1/Clb2 dimers are in the active state. Also, we assume that D affects the threshold concentration $EC50_g$ of Cdk1/Clb2 activation, and we set for simplicity $EC50_g = k_1 D$. Therefore

$$g(S_4) = D\frac{(k_1 D)^m}{(k_1 D)^m + S_4^m},\ D = r_1 \frac{L}{r_2 + L}. \tag{5}$$

For concreteness, we will use the parameter values $m = 3, k_1 = 1/12, r_1 = 6,$ and $r_2 = 4$. Now, given a steady state of the full system (1) and (4) with concentrations $\overline{S_1}, \overline{S_2}, \overline{S_3}, \overline{S_4}, \overline{C}, \ldots$, it is easy to see that $f(\overline{C}) = \overline{S_4}$, and $g(\overline{S_4}) = \overline{C}$. Conversely, for every pair of concentrations $\overline{S_4}, \overline{C}$ such that $f(\overline{C}) = \overline{S_4}$ $g(\overline{S_4}) = \overline{C}$, one can construct a steady state of the full system by using $\overline{C}$ and $\overline{S_4}$ as inputs of the open loop systems (1) and (4) respectively. In this way the point $(\overline{S_4}, \overline{C})$ that intersects the graphs of both $f(C)$ and $g(S_4)$ corresponds to the unique steady state of the system (1), (4). We assume that this equilibrium is locally stable (this depends on the details of the system (4)).
Importantly, we also assume that the convergence towards this steady state is fast with respect to the expression of Clb2.

An ultrasensitive response in Swe1 activation can stabilize steady state concentration of Cdk1/Clb2 in early mitosis

For any concentration L of Clb2, the steady state concentration of C can now be described as $\overline{C}$, where

$$\overline{C}(L) = g(\overline{S_4}, L) = g(f(\overline{C}(L), L).$$

Notice that here we wrote explicitly the dependence of g on the total amount of Clb2. We differentiate this equation with respect to L using the chain rule to obtain $\dfrac{d\overline{C}}{dL} = \dfrac{\partial g}{\partial S_4}\dfrac{df}{dC}\dfrac{d\overline{C}}{dL} + \dfrac{\partial g}{\partial L}$. It follows that

$$\frac{d\bar{C}}{dL} = \frac{\frac{\partial g}{\partial L}}{1 + \left|\frac{\partial g}{\partial S_4}\right| \frac{df}{dC}}. \quad (6)$$

We now need to assume a qualitative property about the functions f and g, which is satisfied within certain parameter regimes. We will assume that the intersection between f and g lies near the threshold values of the two functions, that is, where the slope of both f and g is large. An algebraic condition for this is that the effective kinetic constants K_D and $V_{\max}$ for f and g are within a similar order of magnitude from each other, or more precisely, that

$$0.1V_{\max,f} < K_{D,g} < 0.9V_{\max,f}$$
$$0.1V_{\max,g} < K_{D,f} < 0.9V_{\max,g}.$$

This condition constrains the possible intersection of the two functions, as illustrated in Figure S6.

This shows in what sense a high ultrasensitivity for f or g can help to maintain a relatively constant plateau for $\bar{C}(t)$ in Figure 5A: the higher the ultrasensitivity of f and g, the larger their slope is in this region of interest, and the larger $df / dC(\bar{C})$ and $|dg / dS_4(\bar{S}_4)|$. A high ultrasensitive behavior will therefore decrease $d\bar{C} / dL$ in (6) within the regime of interest.

It can also be seen in Figure S6 that under the assumed parameter conditions $\bar{C}$ is similar to the value of $K_{D,f}$. But this value is linearly tuned by the phosphatase PP2A^{Cdc55} (see previous section), which provides a justification for the assertion that PP2A^{Cdc55} can control the plateau level of active Cdk1/Clb2 for slowly increasing Clb2.

For the construction of f and g in Figure S5 we use the formulas in (2) and (5) respectively. The parameters used are:
$r_1 = 6, r_2 = 4, m = 3, k_1 = 1/12, a_1 / b_1 = a_2 / b_2 = a_3 / b_3 = 1, S_{\text{tot}} = 6$. The dotted $f(C)$ function is simply $S_{\text{tot}} / (1 + C / P)$. In Figure S51, $P = 2$.
The values chosen for L in Figure S52, are $L = 1, 2, 3$. The values chosen for P in Figure 5B are also $P = 1, 2, 3$.

A detailed mechanistic model for systems-level regulation of Cdk1 and Swe1 activity in early mitosis

Finally, we created a model based on the chemical reactions described schematically in Figure 5C and 5D, including the experimental observation that initial phosphorylation of Swe1 on consensus sites by Cdk1 stimulates Swe1 to bind Cdk1/Clb2 and inhibit it by phosphorylation. In the model, the variable Cdk1 represents the active (unphosphorylated)

state of the protein, and $Cdk1_{in}$ represents the inactive state (even when Cdk1 is bound to other molecules). Similarly, Swe1 is modeled to have 8 Cdk1 consensus phosphorylation sites that are phosphorylated distributively and in a specific order. Subindices 0 through 8 are used to indicate the number of phosphorylated sites. Only the most phosphorylated state of Swe1 ($Swe1_8$) is considered to be active. This is based on the observation that Cdk1/Clb2 in crude extracts associates primarily with a single form of Swe1 (Figure 1E). Based on its electrophoretic mobility, this appears to be the active form of Swe1, which suggests that Cdk1/Clb2 must quantitatively phosphorylate Swe1 on the mapped consensus sites to stimulate Swe1 to bind and phosphorylate Cdk1/Clb2. The enzymatic reactions are modeled in a standard way using mass action kinetics and reversible complex formation. The enzymes $PP2A^{Cdc55}$ and Mih1 are assumed to be present at constant levels and to dephosphorylate Swe1 and Cdk1, respectively.

Since we do not know the relationship between specific phosphoforms of Swe1 and quantitated bands in the western blot, we have refrained from using the transition rates measured in Figures 4 and S5 to fit parameters in this detailed mechanistic model. Instead, for simplicity we have used an arbitrary rate equal to one for every chemical reaction. However, we also carried out a parameter robustness analysis in which every parameter was varied over two orders of magnitude at random using logarithmic sampling. The solution using every parameter set we tested converged towards an equilibrium, and moreover the qualitative behavior of Cdk1/Clb2 activity was as described in Figure 5D (transient increase followed by reduction to a lower basal level), irrespective of the choice of parameter values. More generally, the qualitative behavior of the system seems robust to the kind of changes that might occur under widely varying conditions of growth.

An interesting problem related to the evolution of signaling networks is the effect of changing the total number of Swe1 phosphorylation sites. In order to study this question, we systematically changed the number n of phosphorylation sites over a range of different values, using the same parameter values in each case (Figure S7). As n increases, there is a longer delay before the maximally phosphorylated form of Swe1 is produced and inhibits Cdk1/Clb2. We observed a roughly linear increase in the time that the maximal transient concentration of Cdk1/Clb2 is reached. Also, the longer time delay allows for more Clb2 to be produced and to activate Cdk1, which results in a higher maximum transient level of active Cdk1/Clb2 concentration for larger n. Interestingly, to our surprise, the final basal level of active Cdk1/Clb2 remained essentially unchanged for different values of n. In other words, the number of Swe1 phosphorylation sites affects the timing and the amount of active Cdk1/Clb2 that is transiently produced during early mitosis but not its ultimate basal level.

References

Gunawardena (2005) Multisite protein phosphorylation makes a good threshold but can be a poor switch. *Proc Nat Acad Sci USA* **102**(41):14617--14622.

Z. Serber and J.E. Ferrell, Jr. (2007) Tuning bulk electrostatics to regulate protein function.

Cell **128**:441--444.
C.M. Furdui, E.D. Lew, J. Schlessinger, and K.S. Anderson (2006) Activation of FGFR1 kinase is mediated by a sequential and precisely ordered reaction. *Mol Cell* **21**:711--717.

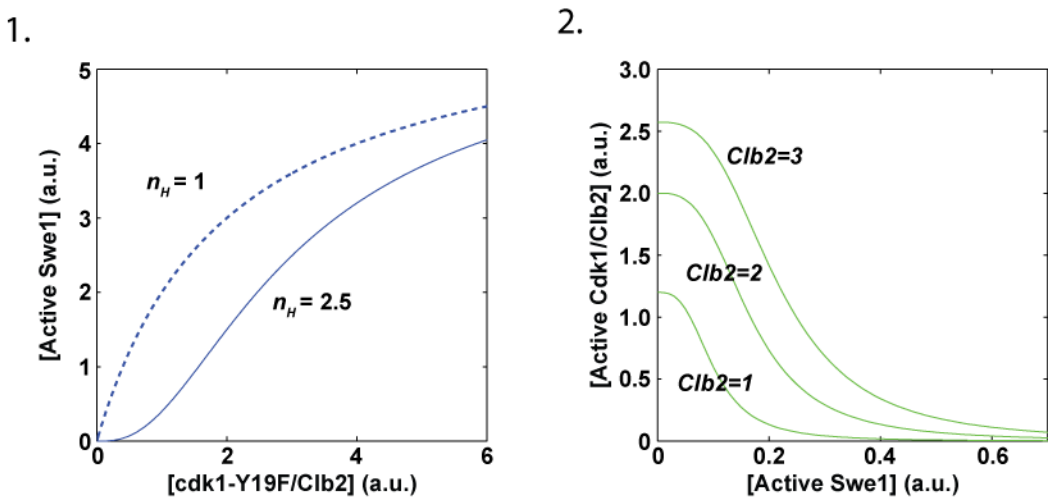

Figure S5: A possible mechanism for the stabilization and control of active Cdk1/Clb2 in early mitosis, through an ultrasensitive response of Swe1 to Cdk1/Clb2 and PP2A^{Cdc55}. 1) The dose-response function $f(C)$. The solid curve is a rescaling of the model fit in Figure 4D (fourth graph), with the same ultrasensitive behavior. The dotted curve is a Michaelis-Menten function with Hill coefficient 1. 2) The function $g(S_4)$, a hypothetical response function of Cdk1/Clb2 to different steady state concentrations of active Swe1, for different concentrations of Clb2, using Hill coefficient 3.

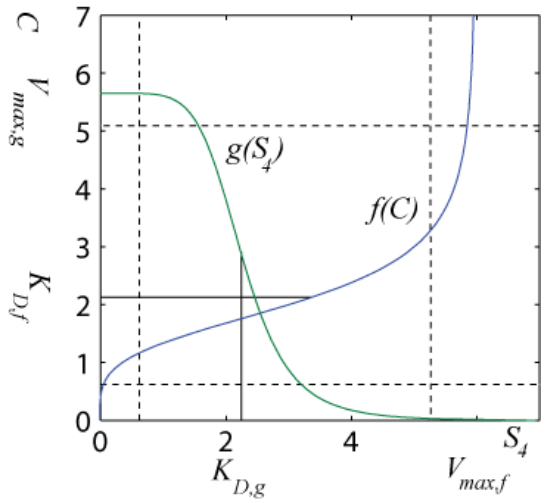

Figure S6: An abstract graph of the functions $g(S_4)$ *and* $f(C)$ *(the latter as a function of the* y*-axis). If* $(K_{D,g}, K_{D,f})$ *lies within the dotted square given by* $V_{\max,f}, V_{\max,g}$*, the intersection of the two graphs tends to lie within their threshold region. In this region, the function* $\bar{C}(t)$ *tends to be more constant given an increased ultrasensitivity in* f*. Also,* $\bar{C} \approx K_{D,f}$*, which is controlled by the concentration* P *of PP2A*^{Cdc55}*.*

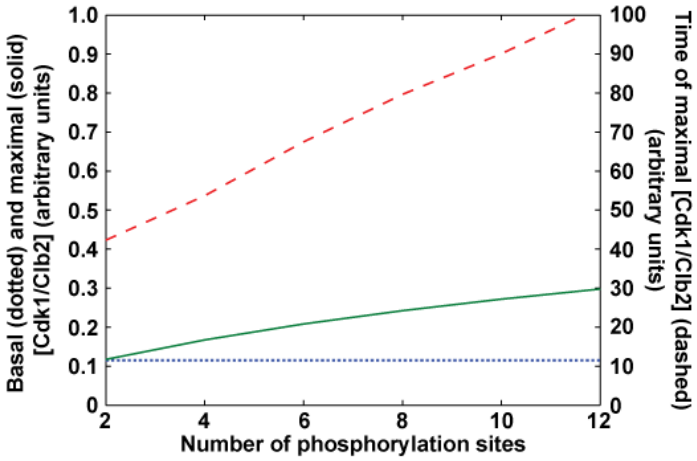

Figure S7: For every value of the total number of phosphorylation sites in Swe1, a simulation such as in Figure 5D was carried out. Displayed are the final (dotted) and maximal (solid) concentrations of active Cdk1/Clb2. Displayed dashed is the time at which the maximal concentration of Cdk1/Clb2 was reached.}